Fizikalna podloga nastanka i kvalitativna karakterizacija slike na CT uređajima

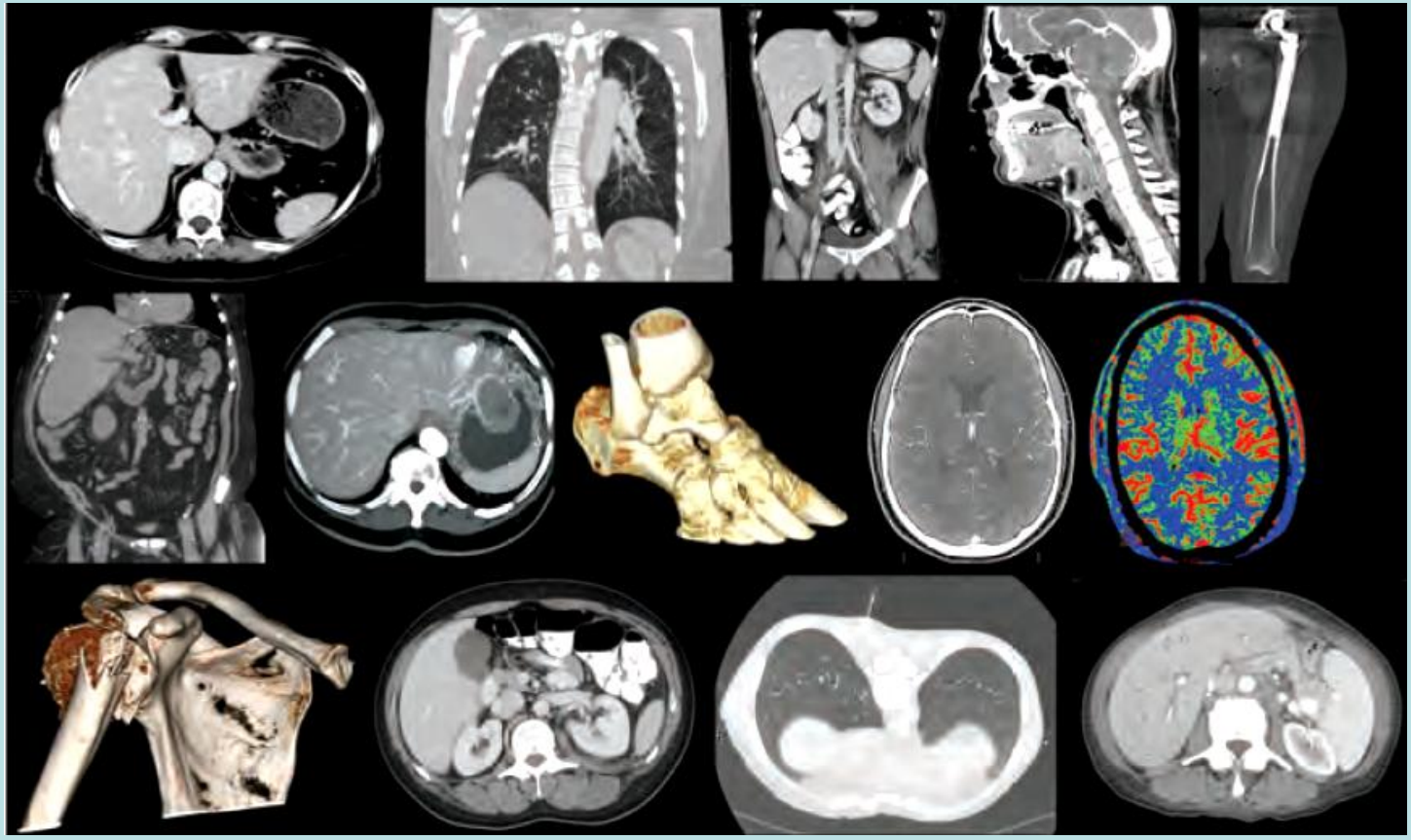

Prof. dr. Marko Radoš, KBC Zagreb

Iznimna kvaliteta slike i brza akvizicija podataka doveli su do velikog porasta korištenja CT u posljednjih 10 godina.

Ključni tehnološki korak bio je uvođenje spiralnog i višerednog detektorskog sustava u CT uređaje.

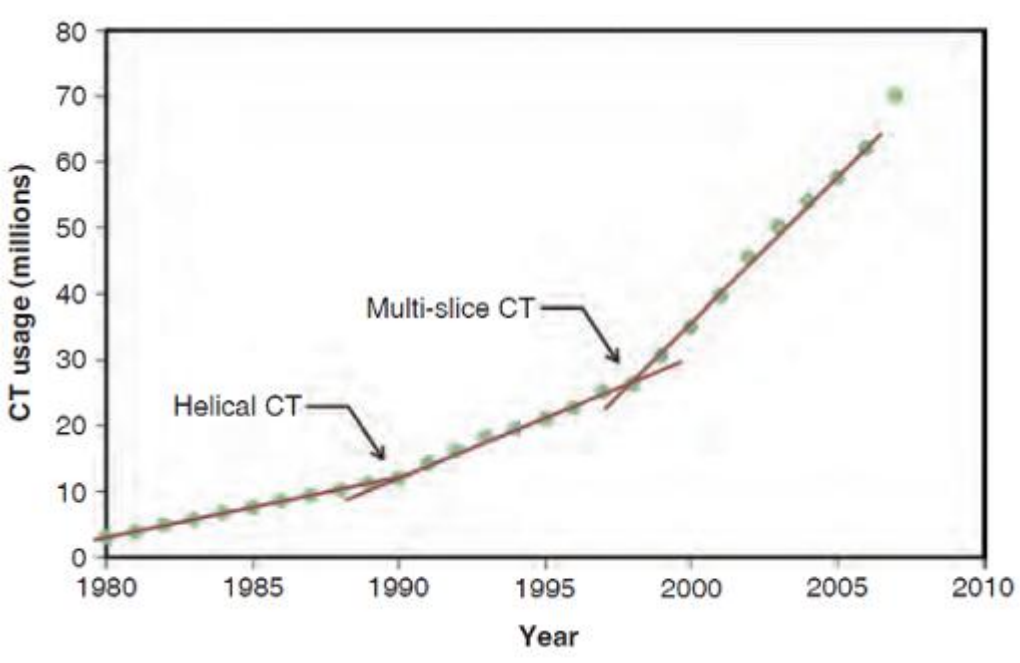

Gantry - Geometrija

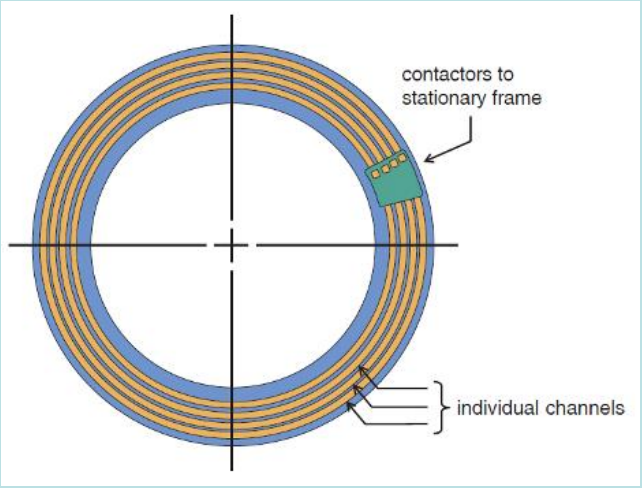

CT slika je krug untar kvadrata s matricom slike 512X512

Površina kruga (FOV) uzduž pacijenta (z) formira volumen cilindričnog oblika.

Većina CT uređaja maksimalni FOV 50 to 70 cm

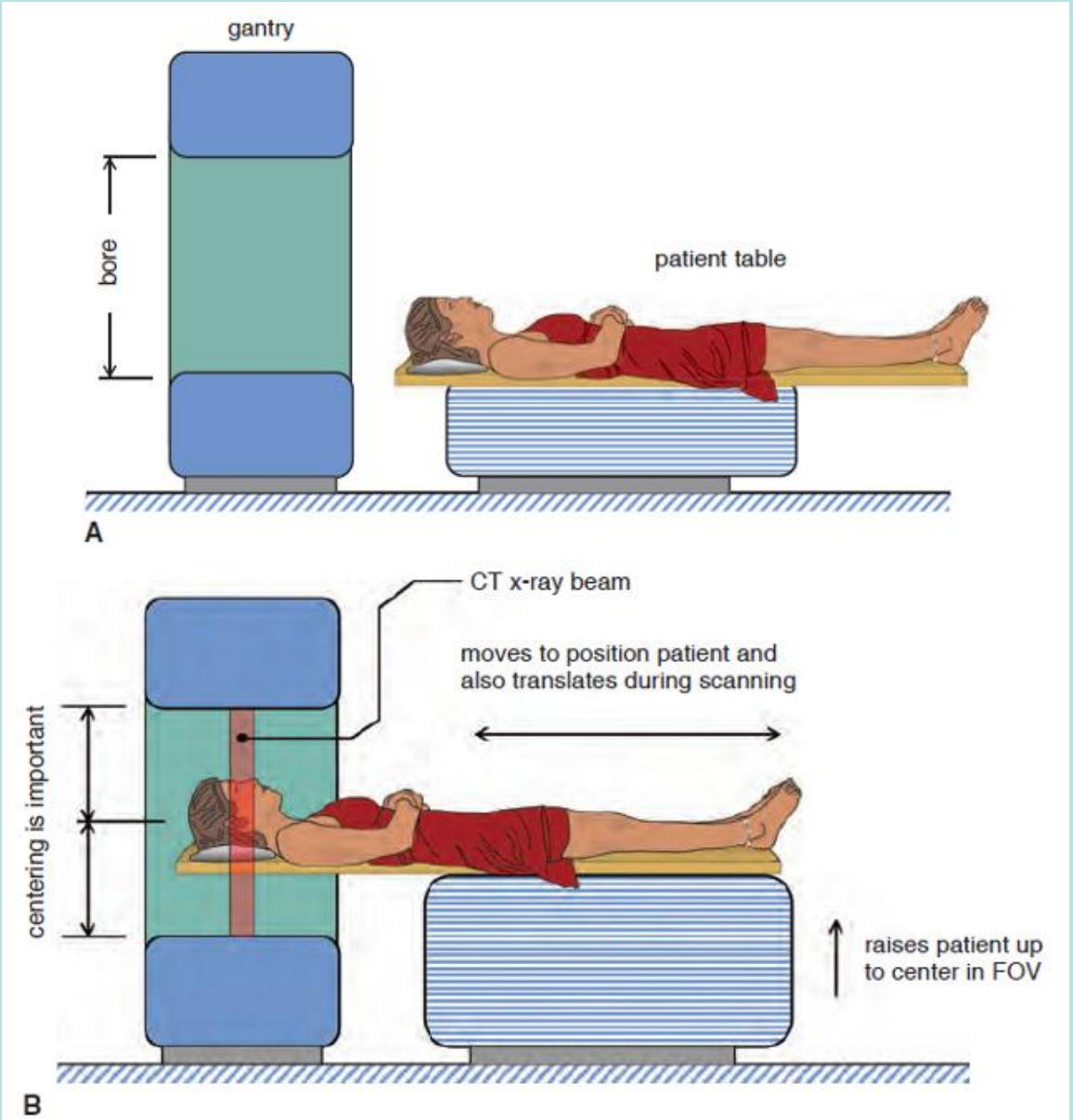

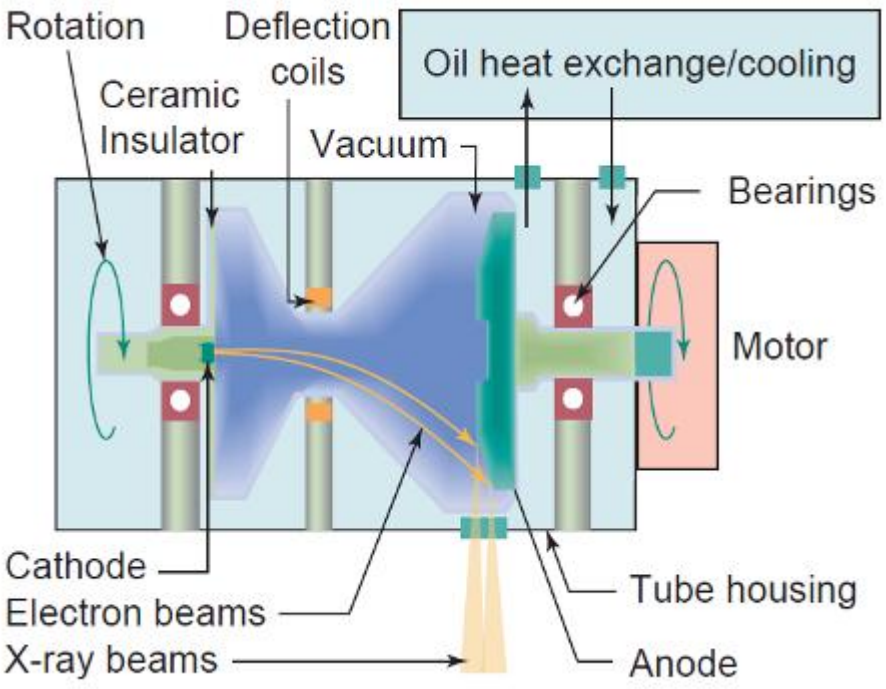

Suvremena rtg. cijev za CT uređaje

-Defleksijske zavojnice magnetski usmjeruju elektronski oblak u ciljnu toču na anodi
-Cirkulirajuće ulje brzo odstranjuje toplinu nastalu u rtg. cijevi.

-Elektronski snop može vrlo brzo izmjnenjivati poziciju žarišne točke
- „flaying focal spot”

Heel Effect

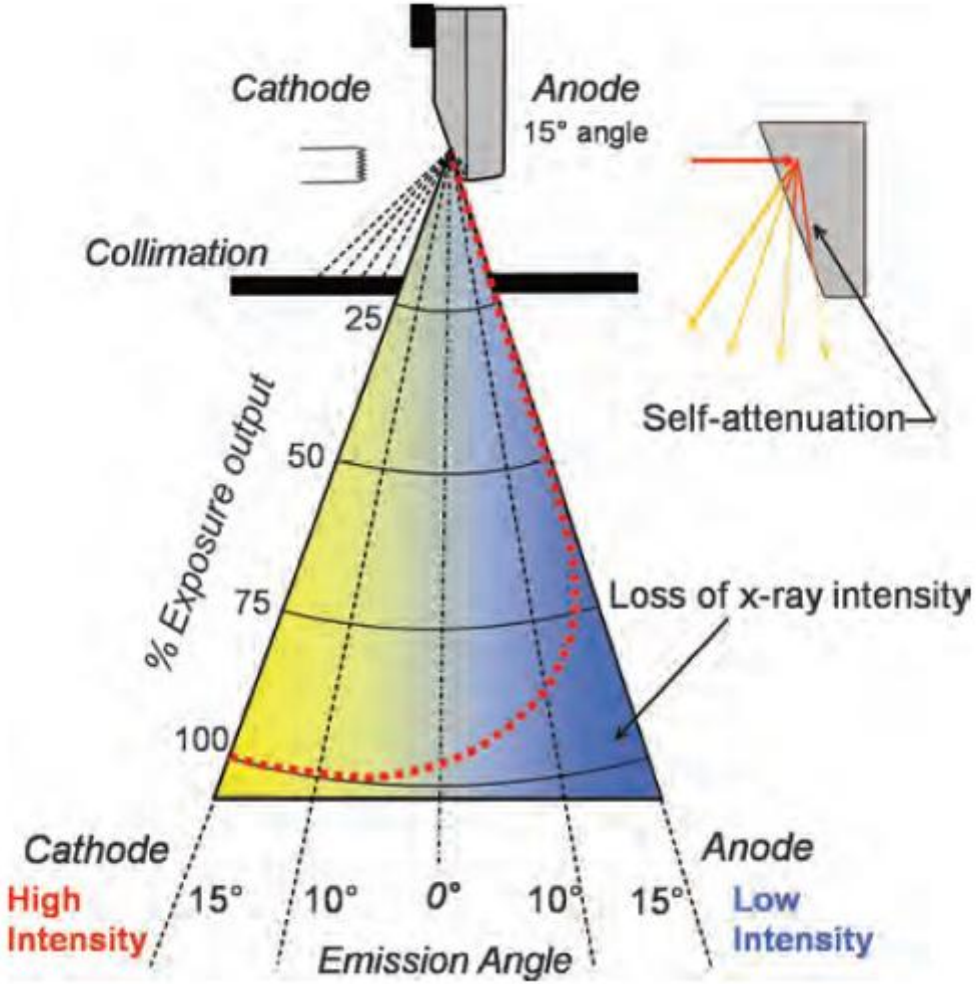

■ FIGURE 6-17 The heel effect is a loss of intensity on the anode side of the x-ray field of view. It is caused by attenuation of the x-ray beam by the anode. Upper right is an expanded view that shows electrons interacting at depth within the anode and the resultant "self attenuation" of produced x-rays that have a trajectory towards the anode side of the field.

Suvremeni višeredni CT uređaji, imaju detektorski sklop od 20-40 cm u z-osi.

Konusna geometrija rtg. snopa.

Moraju se koristiti konusni rekonstrukcijski algoritmi.

lepeza snop (fan beam)

- **Rtg. Zraka**
- **projekcija**

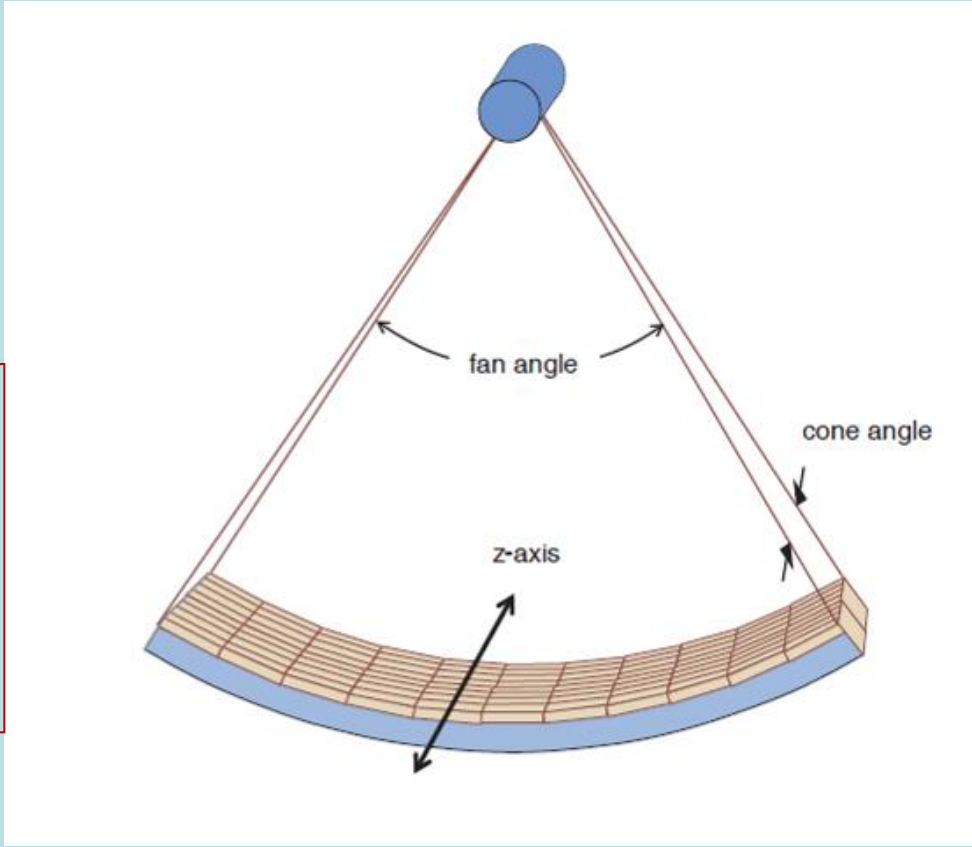

Najnoviji Ct uređaji (nisu još uvijek u širokoj primjeni) koriste flat panel detektore te govorimo o „true cone beam” CT uređajima (angio sale).

Koriste se u radijacijskoj terapiji, dentalnoj radiologiji, radiologiji dojke, radiologiji ekstremiteta SPECT/CT sistemima.

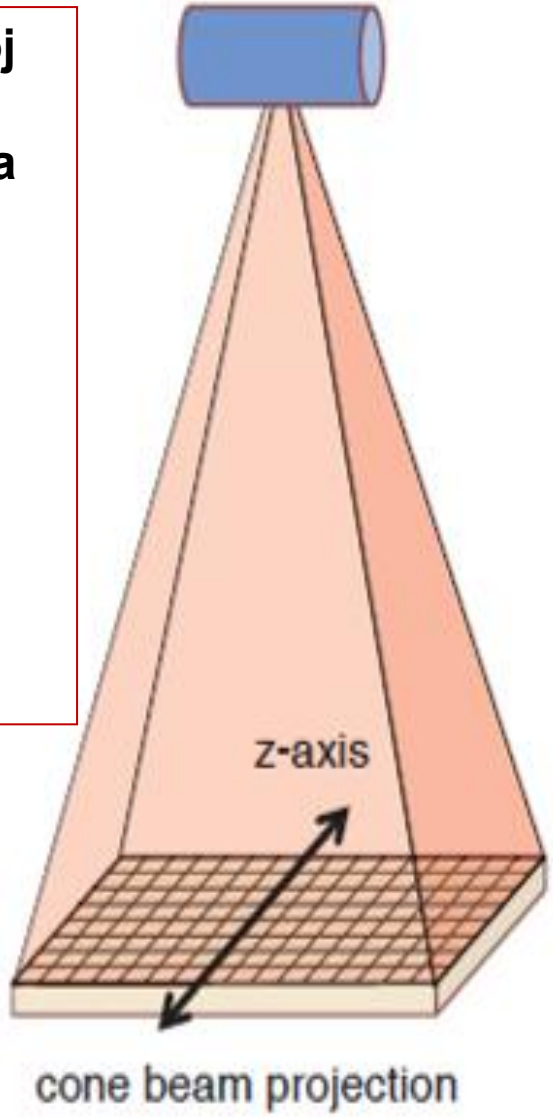

Temeljni koncept i Definicije

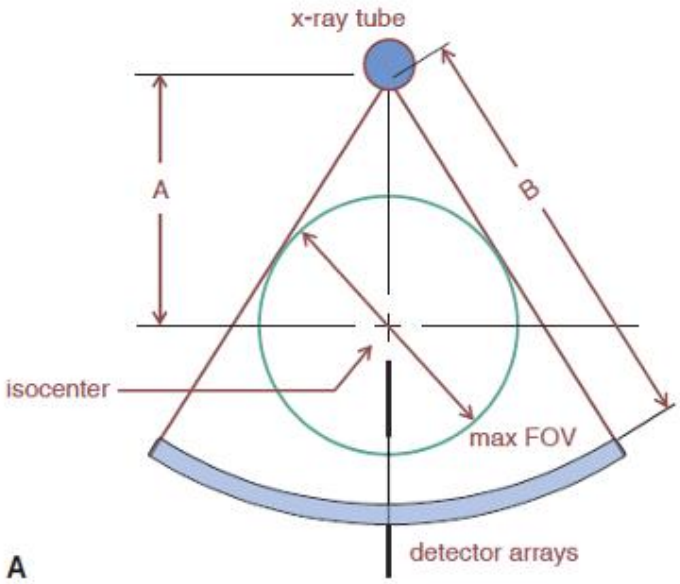

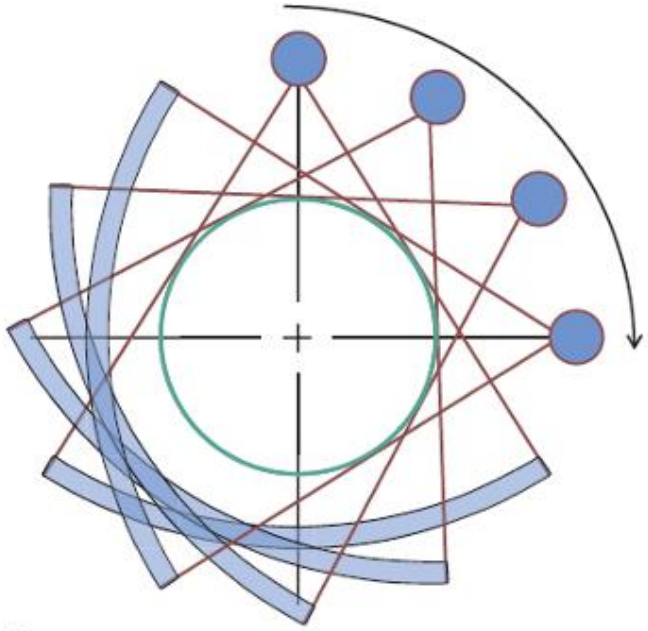

Izvor-izocentar udaljenost, A
Izvor-detektor udaljenost, B
Povećanje, M = B/A

rtg-zraka, cijev, filteri, i kolimacija

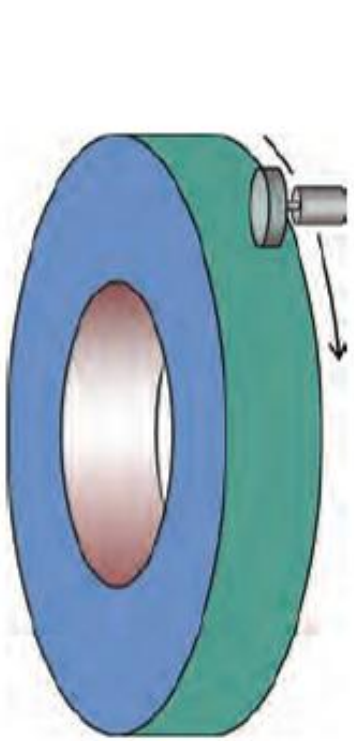

A. tube position relative to gantry

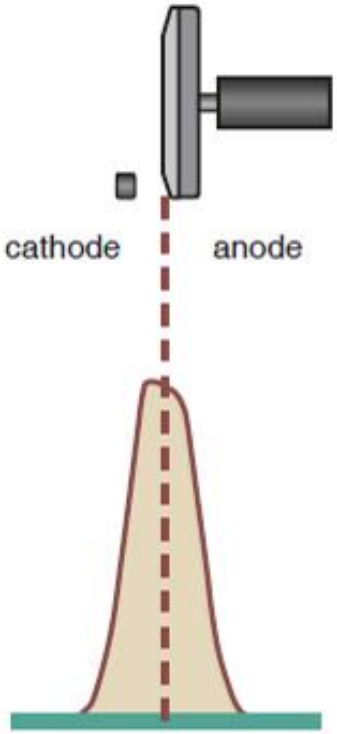

B. X-ray beam profile along z

rtg-cijev rotira zajedno s gentrijem.
Anodno-katodna os je paralelna sa z-osi.
profil rtg-snopa s prikazanim „heel” efektom u z- osi

rtg-zrake, cijev, filteri, i kolimacija

Većina CT uređaja koristi antirasprsnu tehnologiju jednodimenzionalne rešetke. Septe rešetke smanjuju efikasnost snopa (QE). U stvarnosti septe su znatno gušće nego prikazuje slika

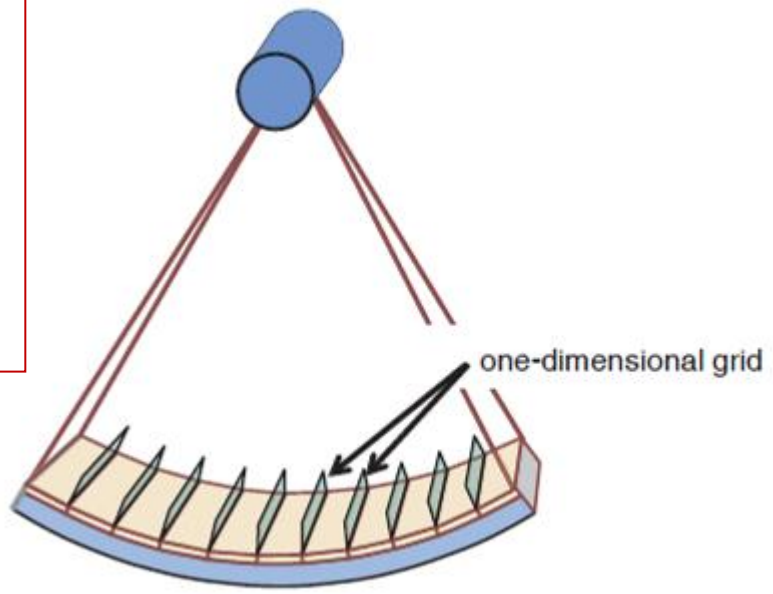

rtg-zrake, cijev, filteri, i kolimacija

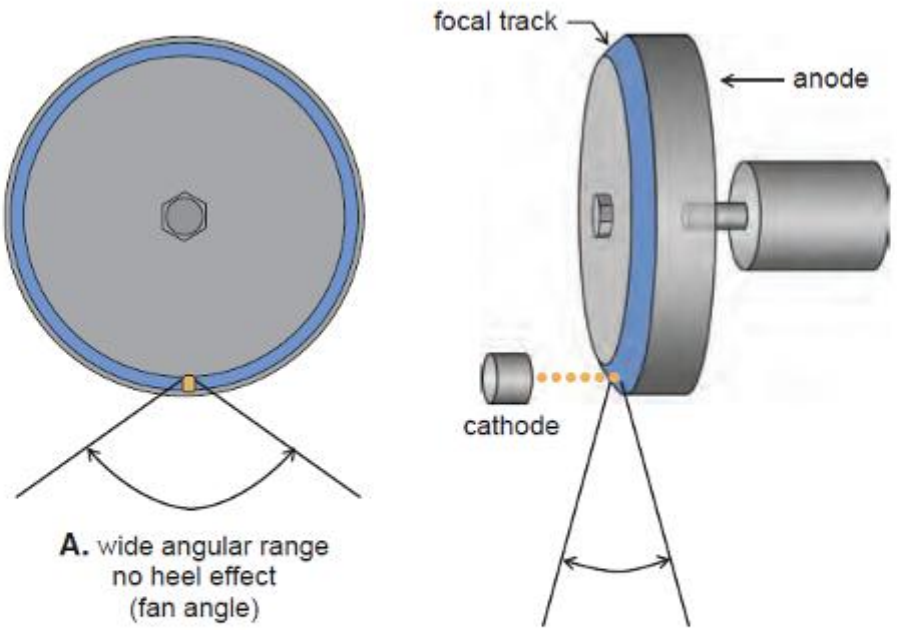

Slika prikazuje kutna pokrivanja rtg-cijevi.
fan-beam kut je širok, a con-beam kut je uzak

rtg-zrake, cijev, filteri, i kolimacija

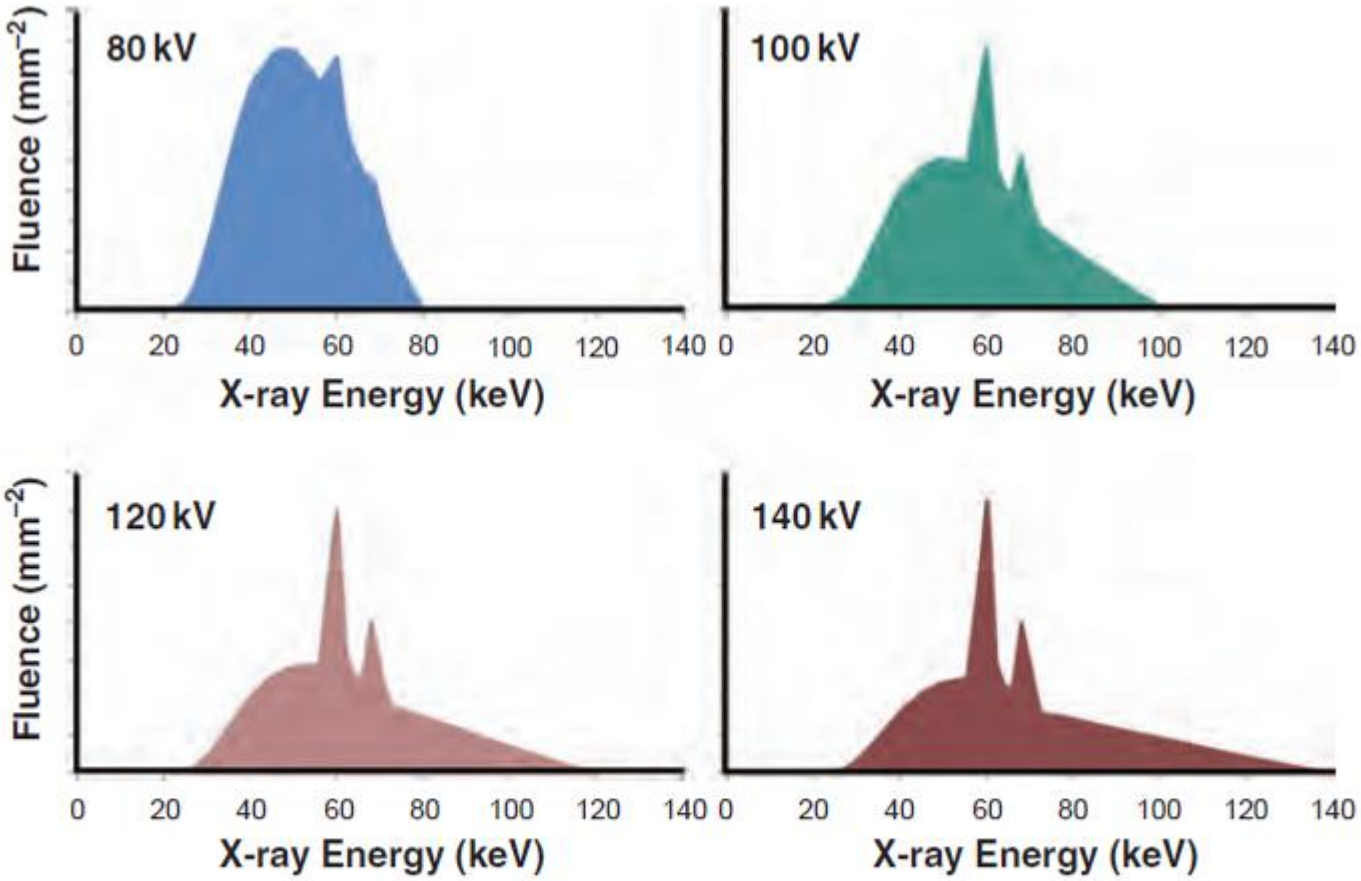

Tipični rtg-spektar, naponi na cijevi 80-140 kV.
Rtg-snop je „otvrdnut” korištenjem filtera (5-10 mm Al).
Također uvijek su u korištenju filteri rtg-profila (shape filteri)

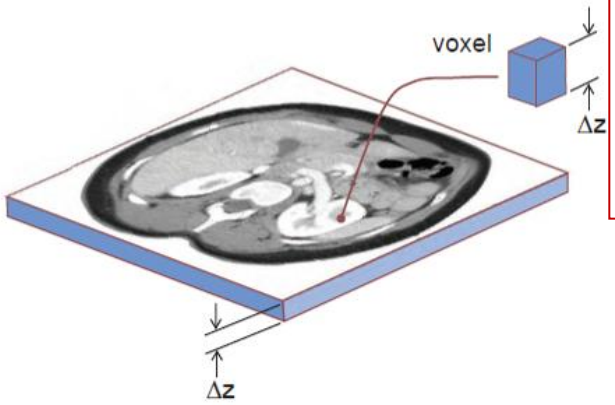

A. in the patient

Dimenzije voxela u ravnini (x,y) i u z-osi, daju volumni element koji je temelj matrične (mozaične) slike. Moderni CT uređaji imaju sve tri dimenzije iste (koncept izotropnosti).

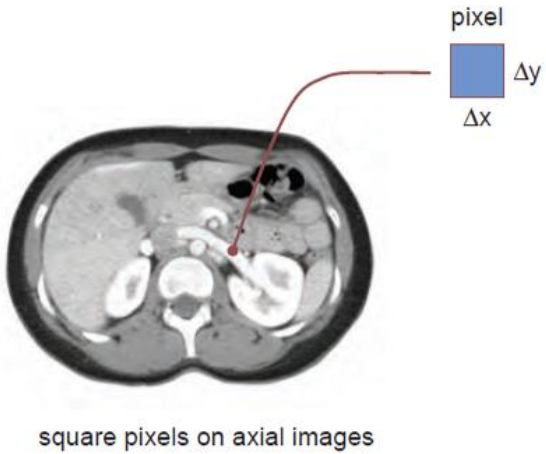

square pixels on axial images

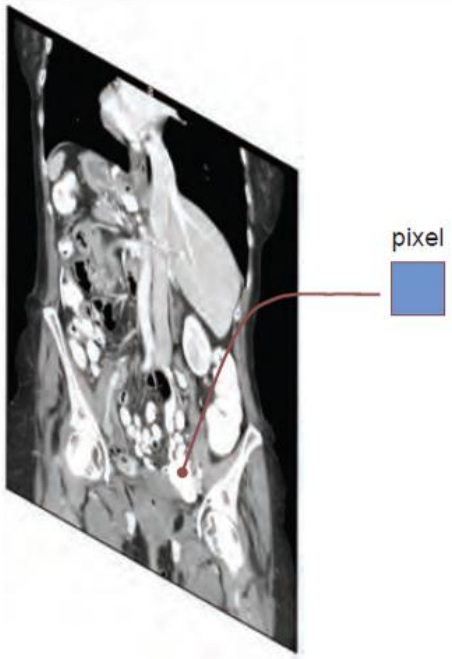

rectangular pixels on coronal images

Bez obzira na 3-dimenzionalnu prirodu CT skeniranja, pojedinačne slike su zapravo 2-dimenzionalne. Kod svih digitalnih slika, svaki slikovni element, pixel odgovara jednom volumnom elemntu (voxel).
Piksel na aksijalnoj slici je kvadrat, a na frontalnoj i sagitalnoj je najčešće pravokutnik. (anizotropni koncept)

Detektorski sklop

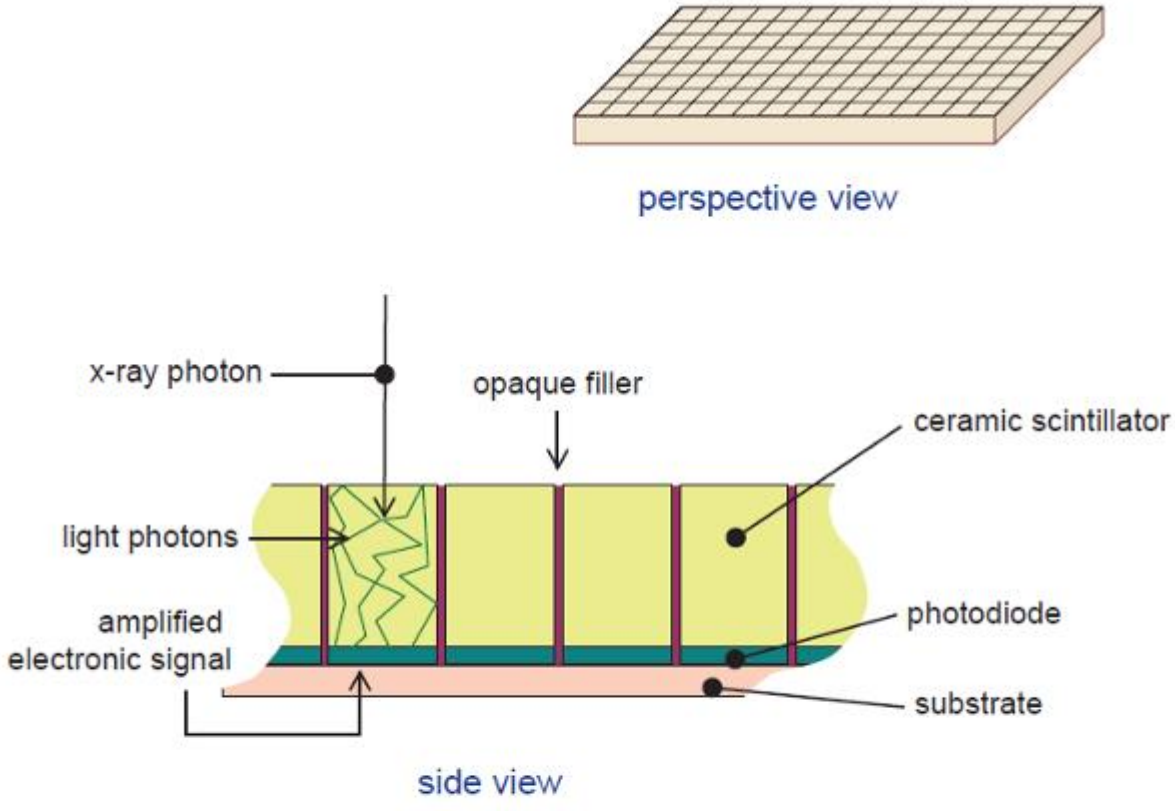

Detektori u suvremenim CT uređajima zapravo su detektorski sklopovi.
Svaki pojedinačni detektor (keramički kristal, UFC) uklopljen je sa fotodiodom koja leži na elektroničkom sklopu (array peocesor). Između detektora je svojevrsni izolator (jaki apsorber fotona) koji sprečava međusobu izmjeni fotona između pojedinih detektora. CT detektori su puno skuplji od radiografskih detektora.

Detektorski sklop

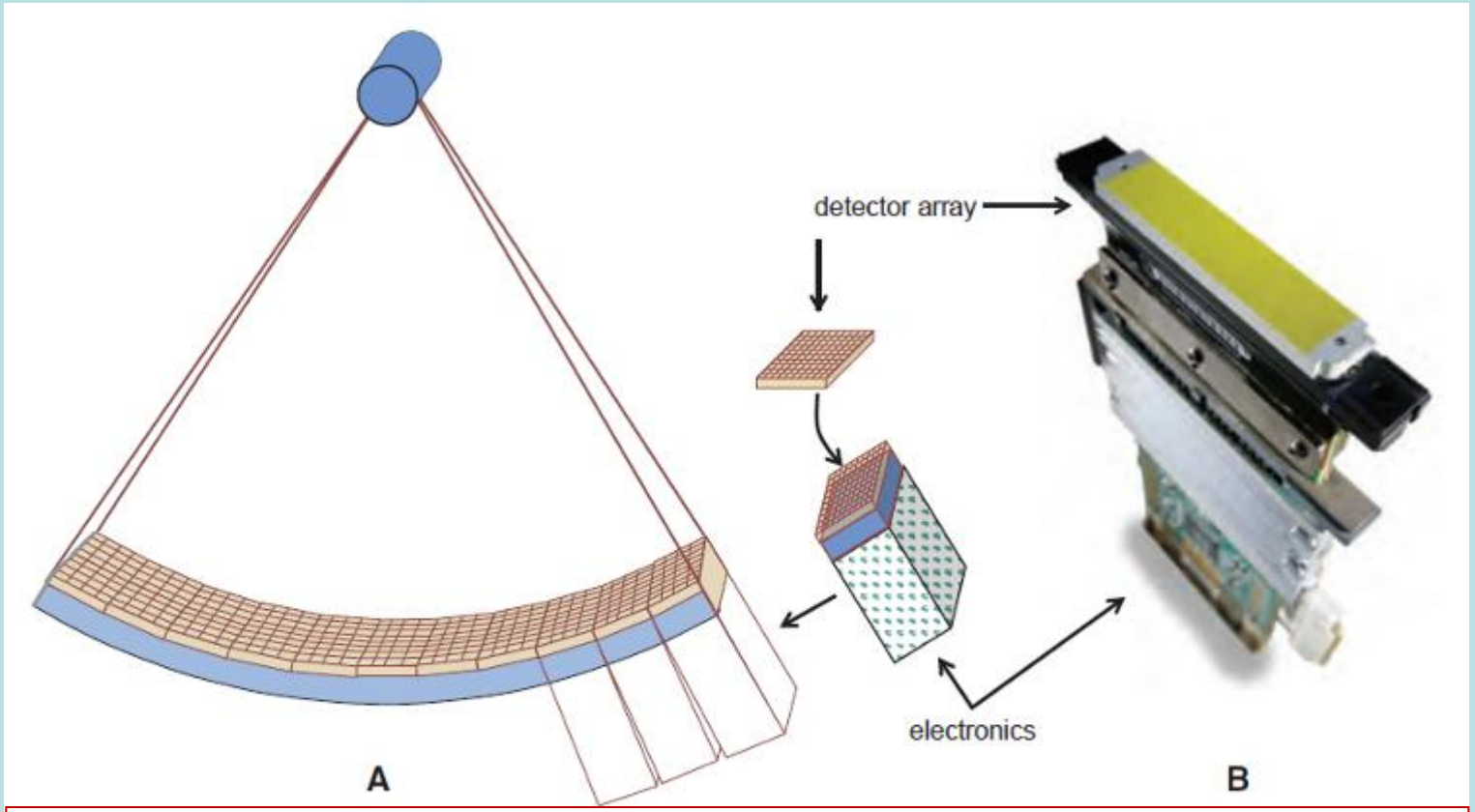

Detektorski sklop je montiran na elektroničkom modulu koji uključuje: napajanje za pojačala, amplifikacijski krug za detektorski modul, analogno-digitalni konverter, etc...

Detektorski sklop

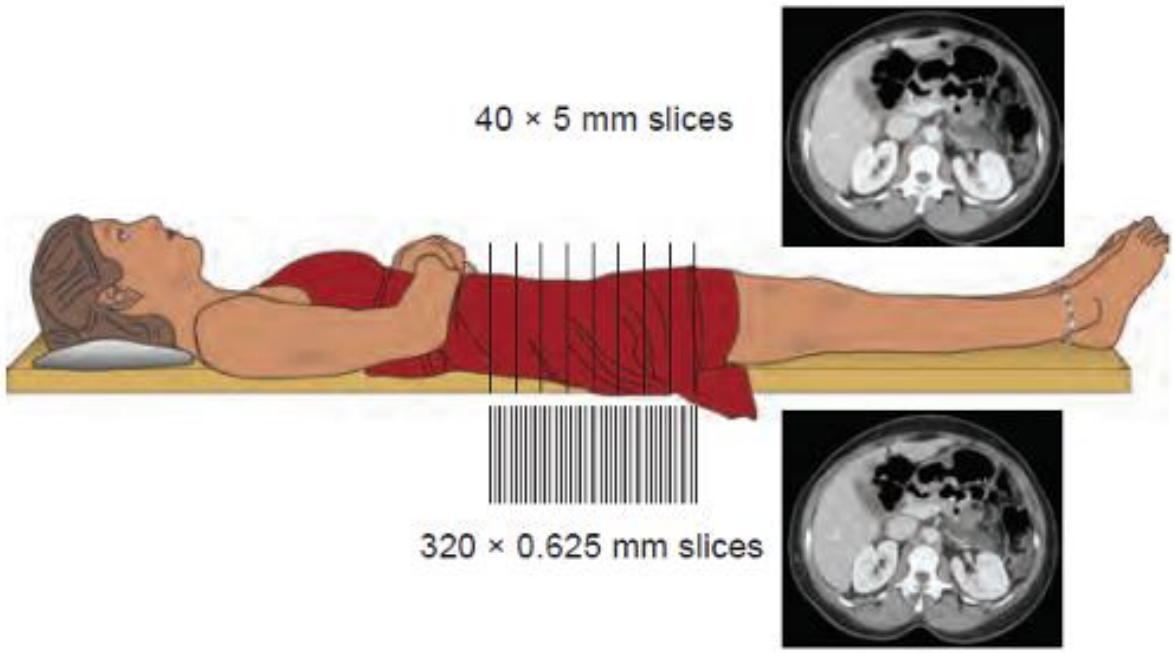

Debljina sloja igra vrlo važu ulogu odnosa radijacijske doze i šuma u slici.
Premda većina CT uređaja može ”snimiti vrlo tanke slojeve”, trebamo postići optimalnu debljinu sloja prema očekivanoj patologiji. Tanki slojevi (0,5 mm) povećavaju bitno šum na slici i višestruko povećavaju dozu koju dobija pacijent.

Doza i šum slike, posljedice tankih slojeva

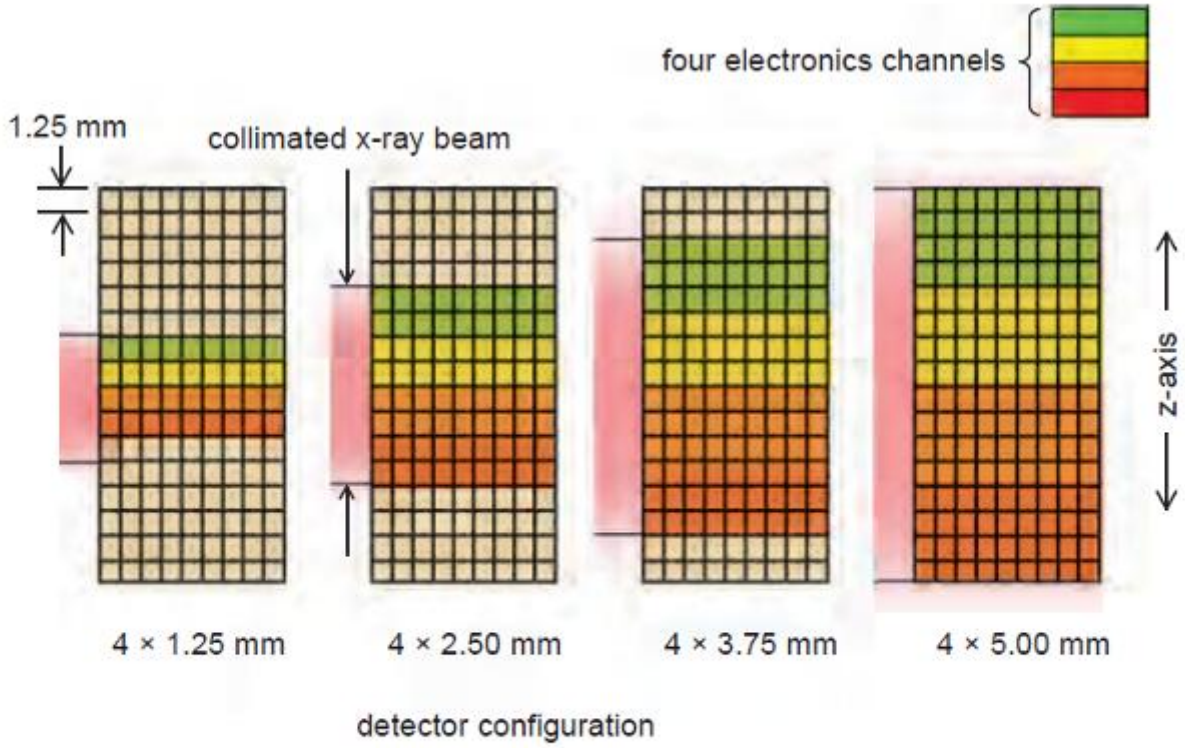

■ FIGURE 10-30 For the early MDCT systems, the number of electronics channels was less than the number of detector arrays, and so a decision of CT slice thickness had to be made *prior* to acquisition. For a standard 16-slice CT scanner as illustrated here, with 4 channels of electronics, the detectors could be used individually (4 × 1.25 mm data sets) or could be binned to produce thicker slices and better CT coverage (e.g., 4 × 5.0 mm data sets).

CT Perfuzija

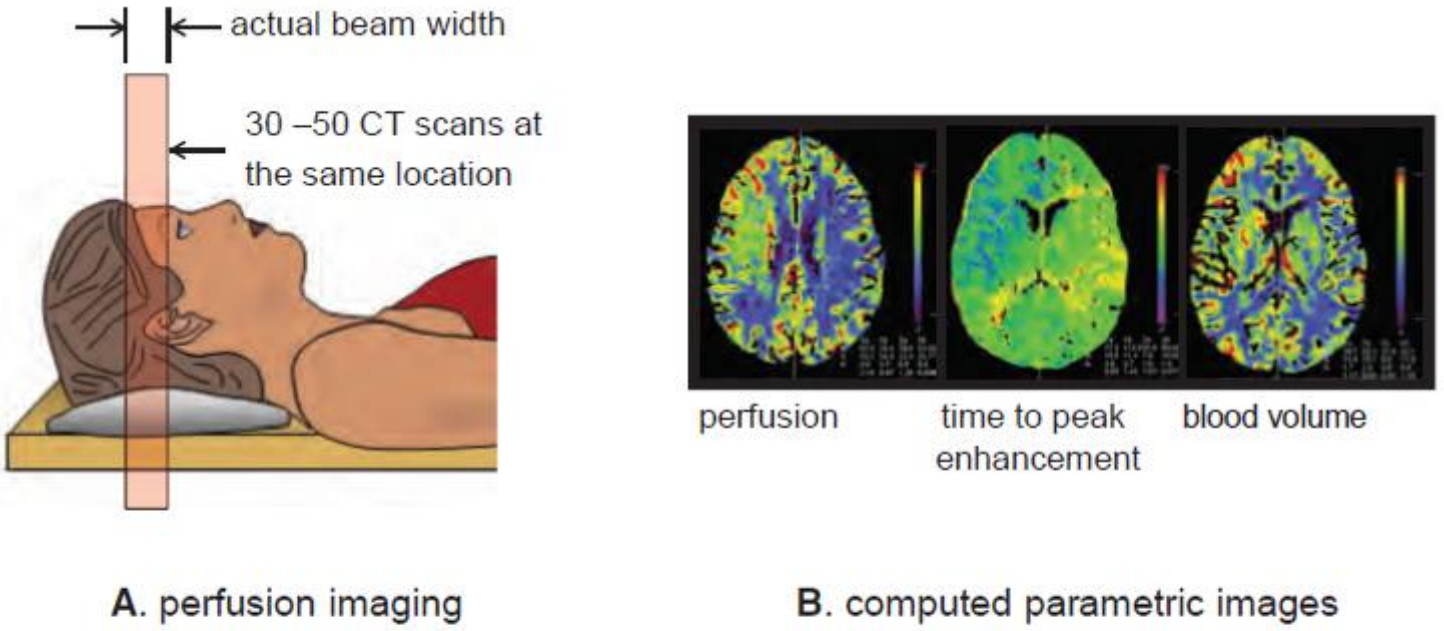

■ FIGURE 10-42 CT perfusion is an extension of CT angiography, where a relatively long time sequence of repeated CT images is acquired for physiologic assessment of various organs (**A**). Typically on the order of 40 full CT data sets are acquired for brain perfusion studies, requiring about 40 seconds. From these data and some user input, (**B**) physiological metrics such as vascular perfusion, time to peak enhancement, and blood volume can be computed using software designed for this purpose.

CT Perfuzija

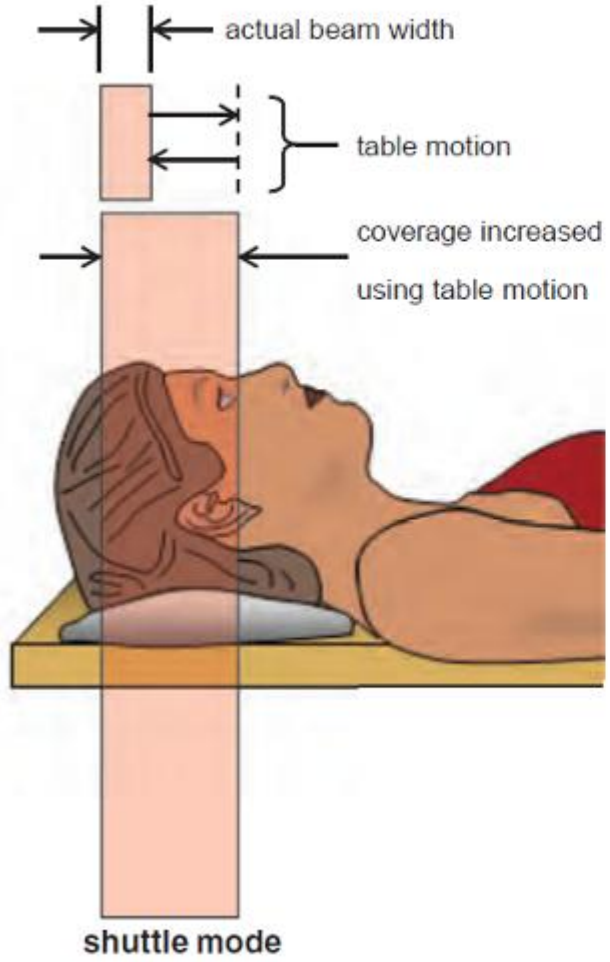

■ **FIGURE 10-43** Shuttle mode imaging is a hybrid between CT perfusion and helical CT imaging—the table shuttles back and forth over a relatively small (e.g., 100 to 200 mm) predefined region in the patient, allowing temporal imaging and hence CT perfusion assessment to be made over a wider length of anatomy than the width (*nT*) of an MDCT field of view.

Modulacija doze

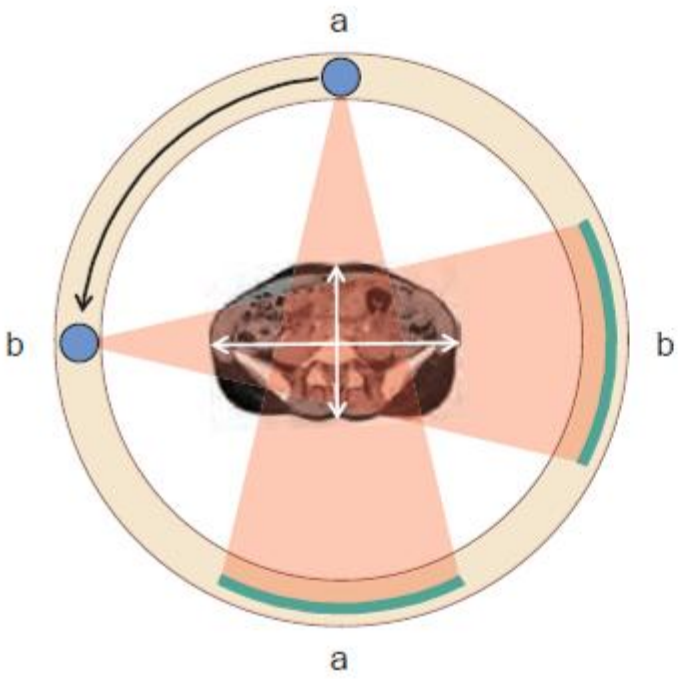

A. Tube rotation around oval patient

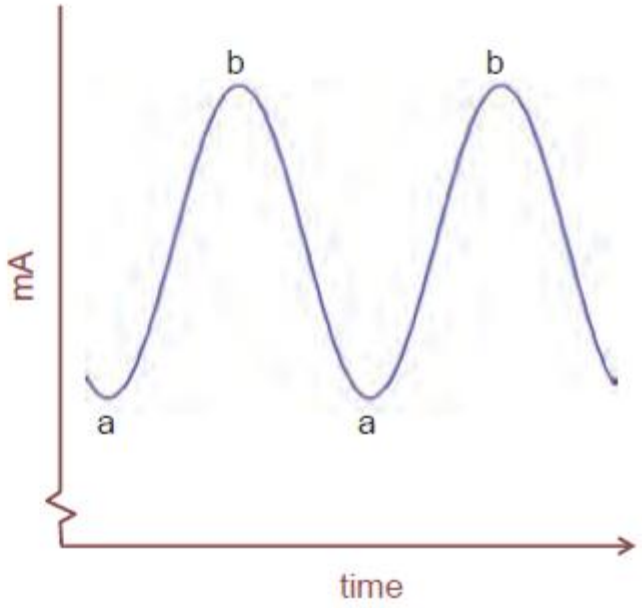

B. mA modulation

■ **FIGURE 10-44** Tube current modulation is illustrated. **A.** As the x-ray tube and detector array rotate around the patient, the x-ray path length is determined either by attenuation measurements or from the CT radiograph, or both. The tube current (mA) is modulated to optimize the use of radiation in the patient. The mA is increased when the beam is projected through thicker regions, and it is decreased as the x-ray beam traverses thinner projections through the patient. **B.** For an elliptical shaped body part such as in the pelvis, the mA modulation scheme is approximately sinusoidal as the gantry rotates around the patient.

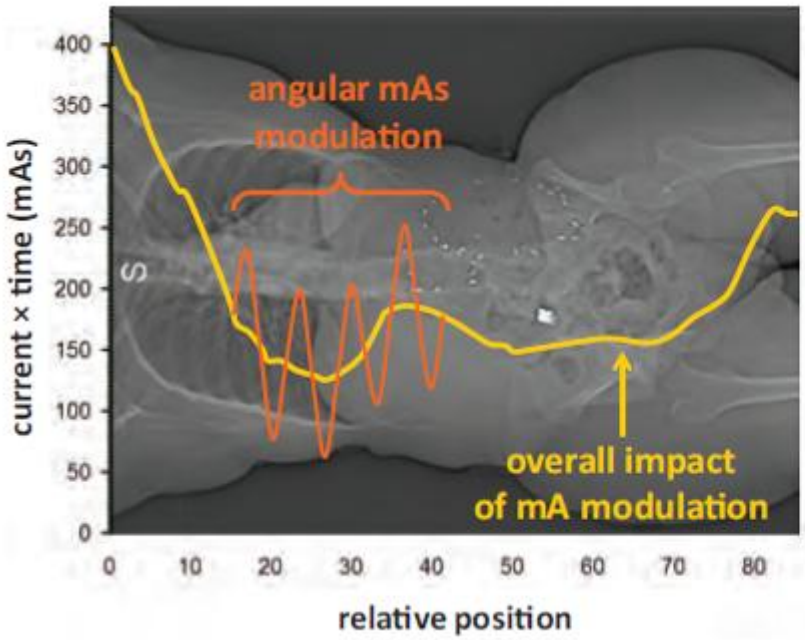

■ **FIGURE 10-45** Tube current modulation occurs as the gantry rotates around the patient to address the different x-ray path lengths between the AP and the lateral projections, but it also is active along the z-dimension of the patient. As the scanner images the patient's thorax, abdomen, and pelvis, the tube current is modulated to optimize the image quality through the entire extent (along z) of the patient scan. The overall mAs per slice along the z-axis of the patient is shown in this figure, and the oscillatory nature of the angular mAs modulation is also shown. (Courtesy SE McKenney.)

CT Protokol

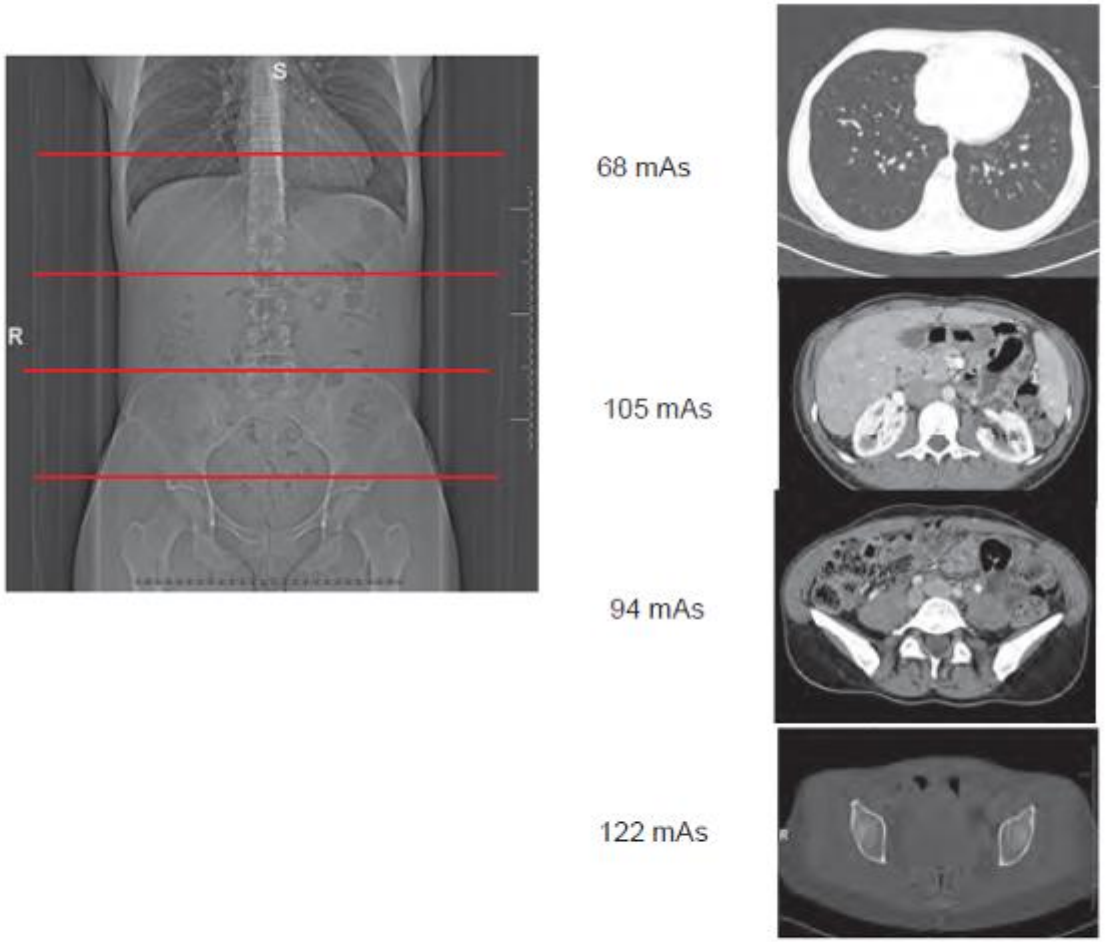

■ FIGURE 10-46 The overall effect of tube current modulation is to use different radiation levels for regions in the body with different overall attenuation, and most tube current modulation schemes result in a more homogeneous distribution of CT noise in the patient images along the z-axis. Here, the mAs values used for the various body regions are indicated.

Rekonstrukcija slike

Preprocessing

Simple Backprojection

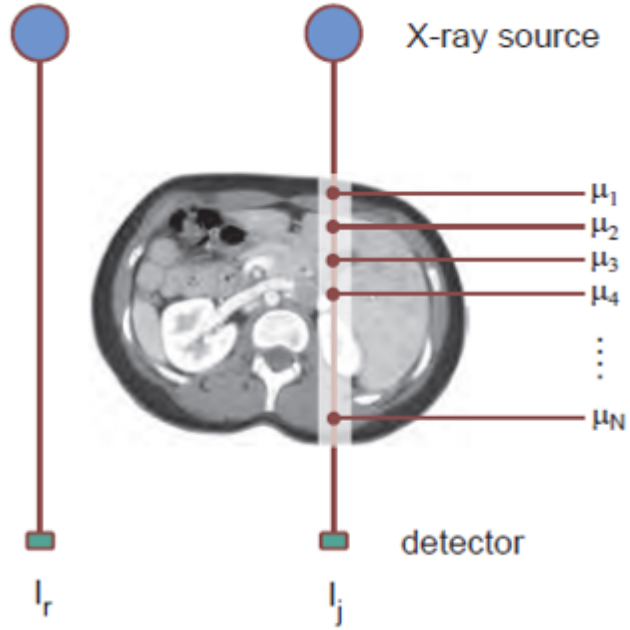

■ **FIGURE 10-47** The reference detector is positioned to detect the output of the CT scanner with no patient anatomy in the measurement, resulting in I_r. A large number of ray measurements I_j are made for detector elements j = 1, N. The ray measurements sample a number of individual linear attenuation (μ) values along the beam path, as illustrated. While x-ray attenuation is an exponential process, logarithmic processing as described in the text converts the measured data to linear projections of μ.

Filtered Backprojection

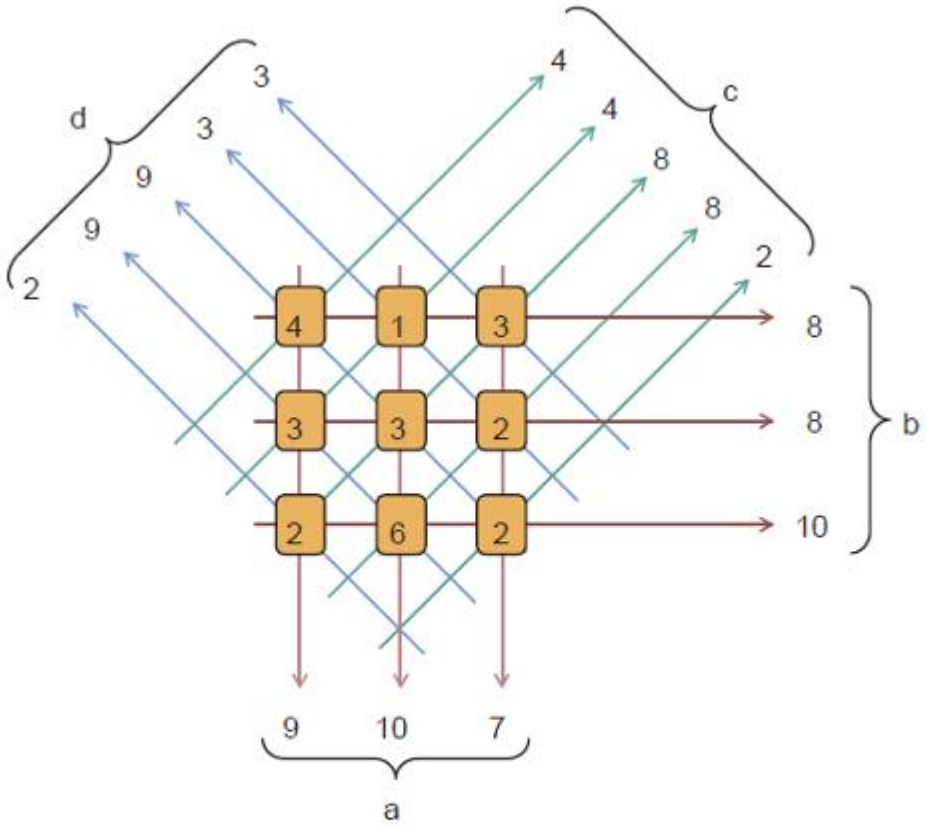

■ **FIGURE 10-48** The 3 × 3 grid in the center of this figure represents the actual attenuation values (scaled to integer values for demonstration), and the projection data (***a, b, c***, and ***d***) show how the attenuation values are summed in this very simplified example. The ***a–d*** projections are the acquired data in a CT scan, and the reconstruction challenge is to determine the values in the nine elements in the 3 × 3 grid. For this simple example, the process is similar to Sudoku. The reader is challenged to use the projection values (only) to find a solution for the values in the gold rectangles.

Filtered Backprojection

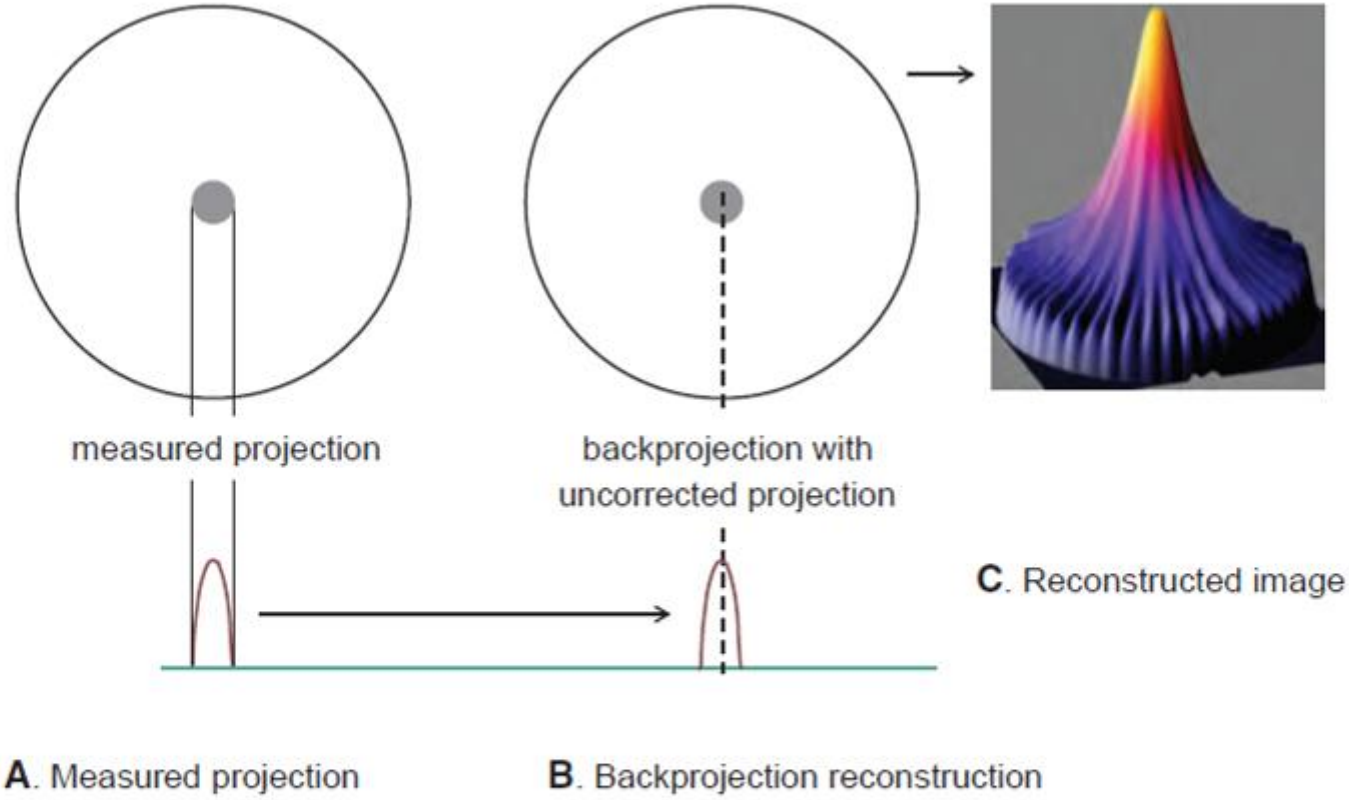

■ FIGURE 10-49 For actual CT data sets, the challenge is to reconstruct a total of 206,000 cells ($\pi \times 256^2$). In this figure, a simple circle at the center of the image is "imaged," producing the *measured projection* in **A**. If these same measured projection data are used in backprojection (**B**), the image will experience a characteristic 1/r blurring as illustrated in **C**.

Filtered Backprojection

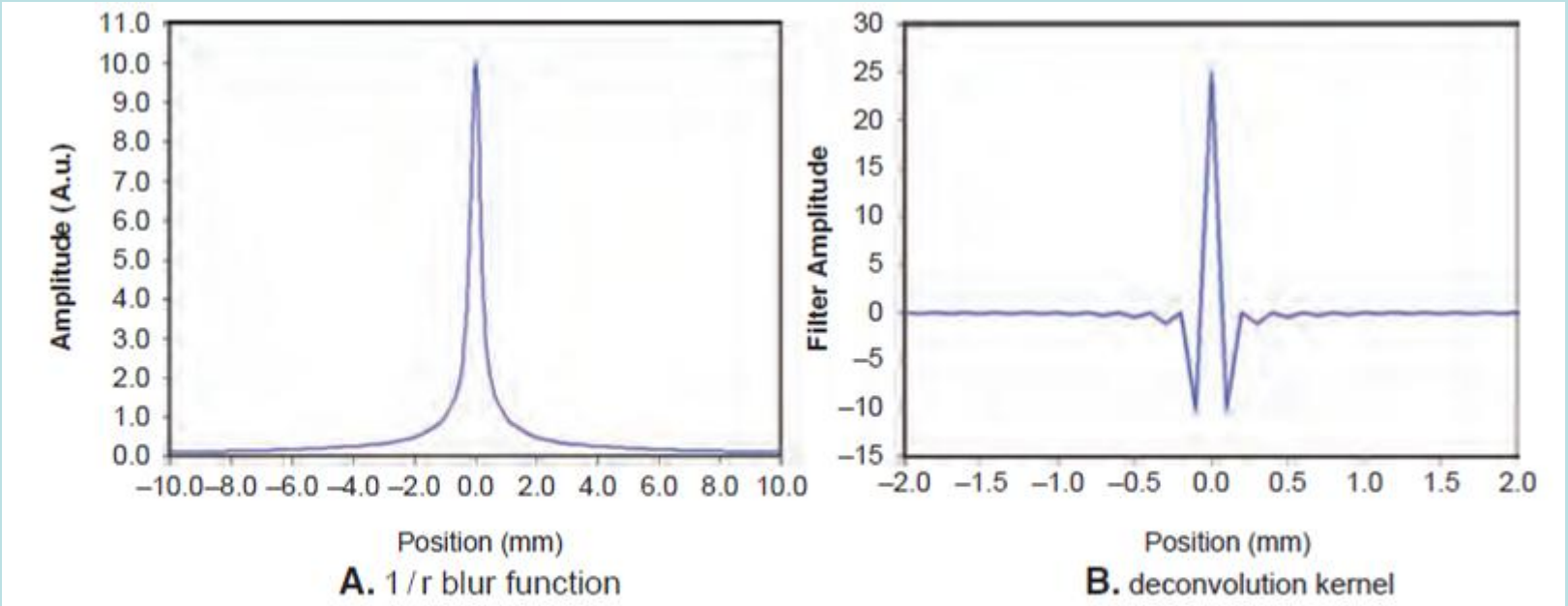

■ FIGURE 10-50 **A.**The 1/r blurring function is illustrated. The blurring caused by the geometry of backprojection can be corrected by deconvolving the measured projection data prior to backprojection, resulting in the process of *filtered backprojection*. **B.** The discrete implementation of the deconvolution kernel is illustrated.

Fourier-Based Reconstruction

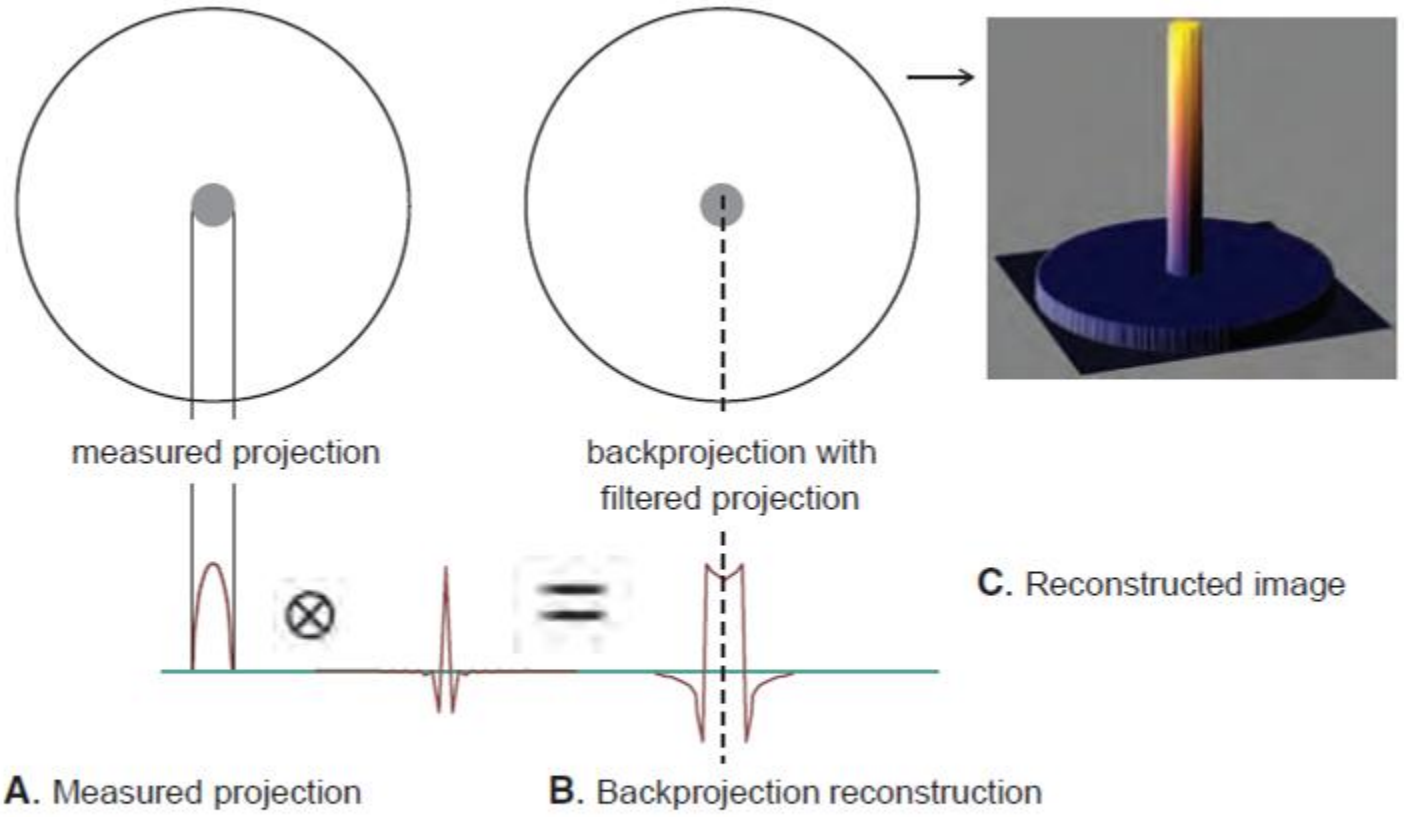

■ FIGURE 10-51 This figure shows the same object and projection data (**A**) as with Figure 10-49A; however, here the measured projection data are deconvolved with the kernel illustrated in Figure 10-50B. The resulting filtered projection data (**B**) are used for backprojection, and this results in an image that reflects the properties of the original object (**C**).

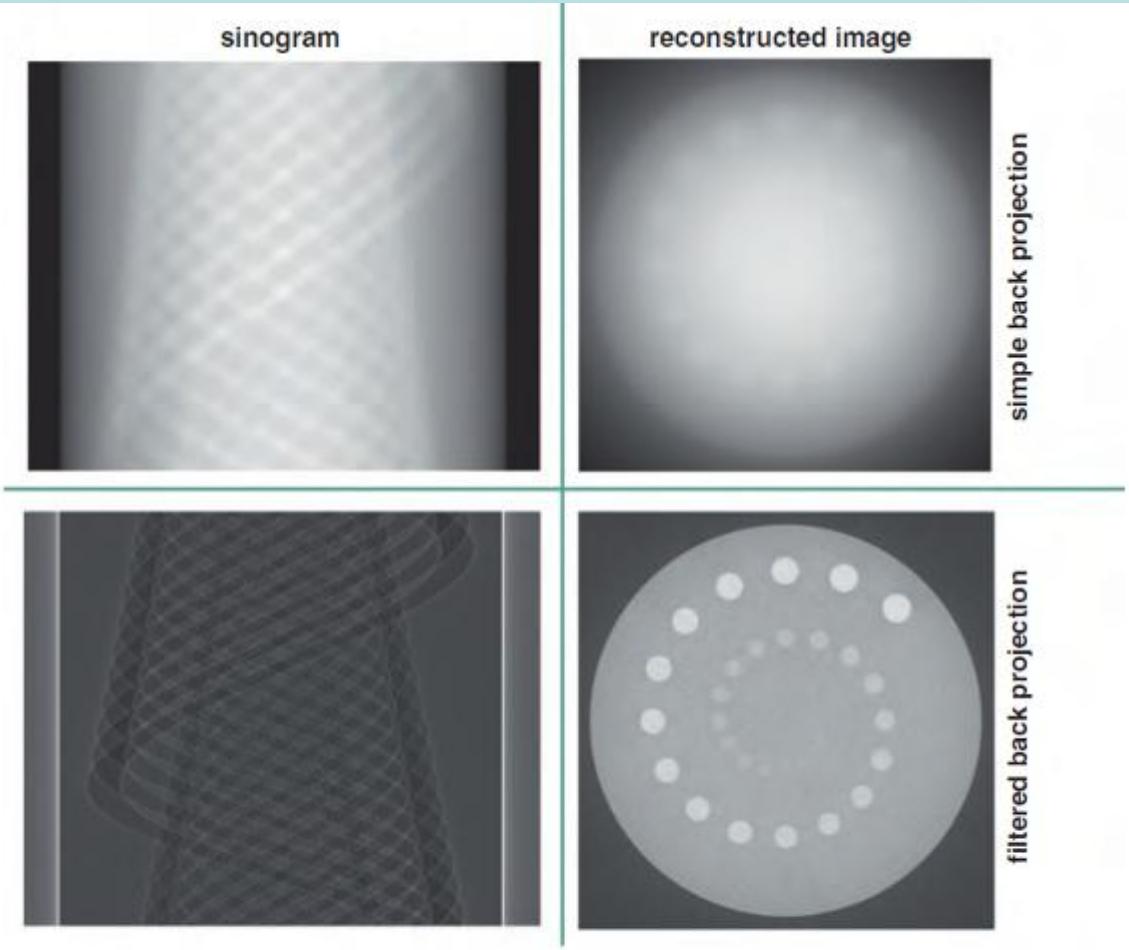

■ FIGURE 10-52 The properties of simple backprojection (top row) and filtered backprojection are illustrated, (bottom row). The sinogram—the plot of the raw data showing rays horizontally and angles vertically—is shown on the left; the sinogram on the bottom has been filtered (horizontally) and the high-pass characteristics of the filtering process are evident. Backprojection of the filtered sinogram data results in an image that closely matches the characteristics of the object that was scanned, while the upper reconstructed image shows significant blurring.

Iterative Reconstruction in CT

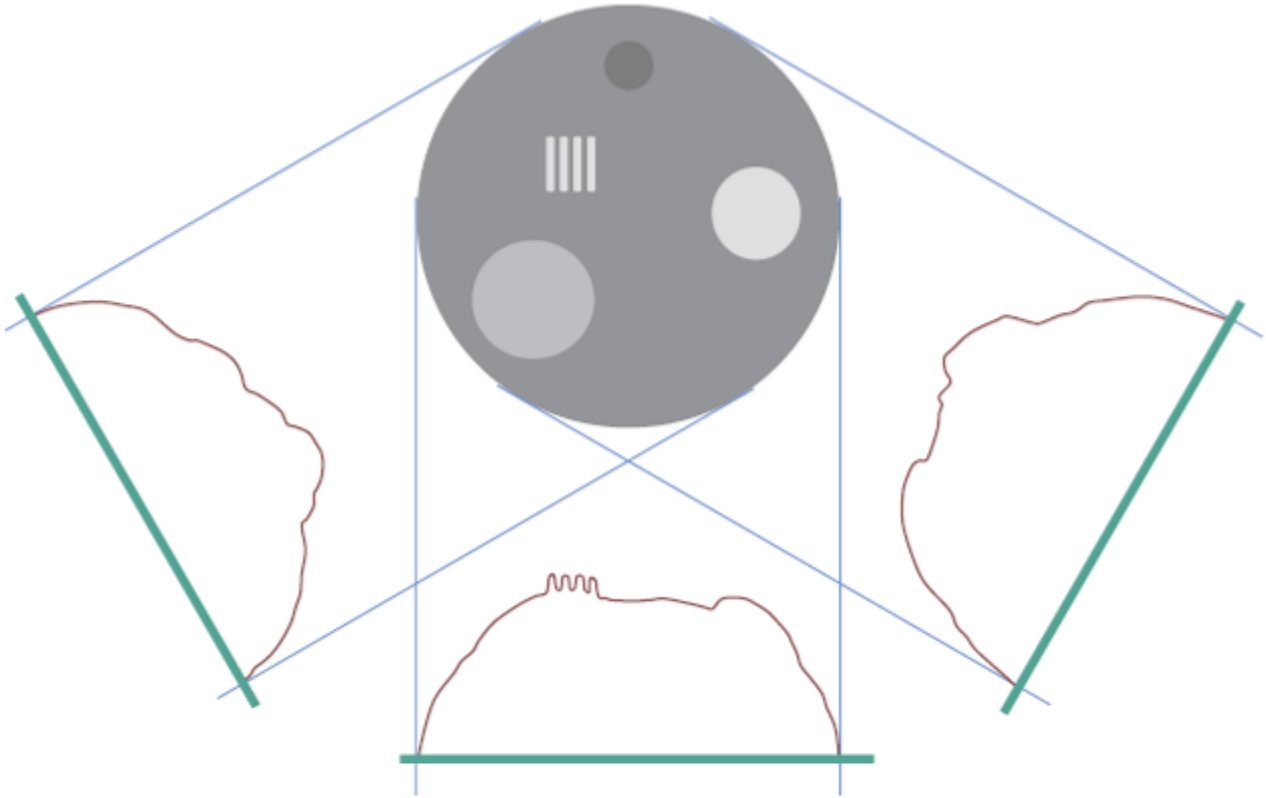

■ **FIGURE 10-54** This figure shows an object and three projections through the object, illustrating a small subset of the measured projection data acquired during CT scanning. These projection data are in principle physically measured using the detector hardware on the scanner, but if a guesstimate of the image data is known, the projections can also be computed (as forward projections) using relatively simple mathematics (sines and cosines) in a computer.

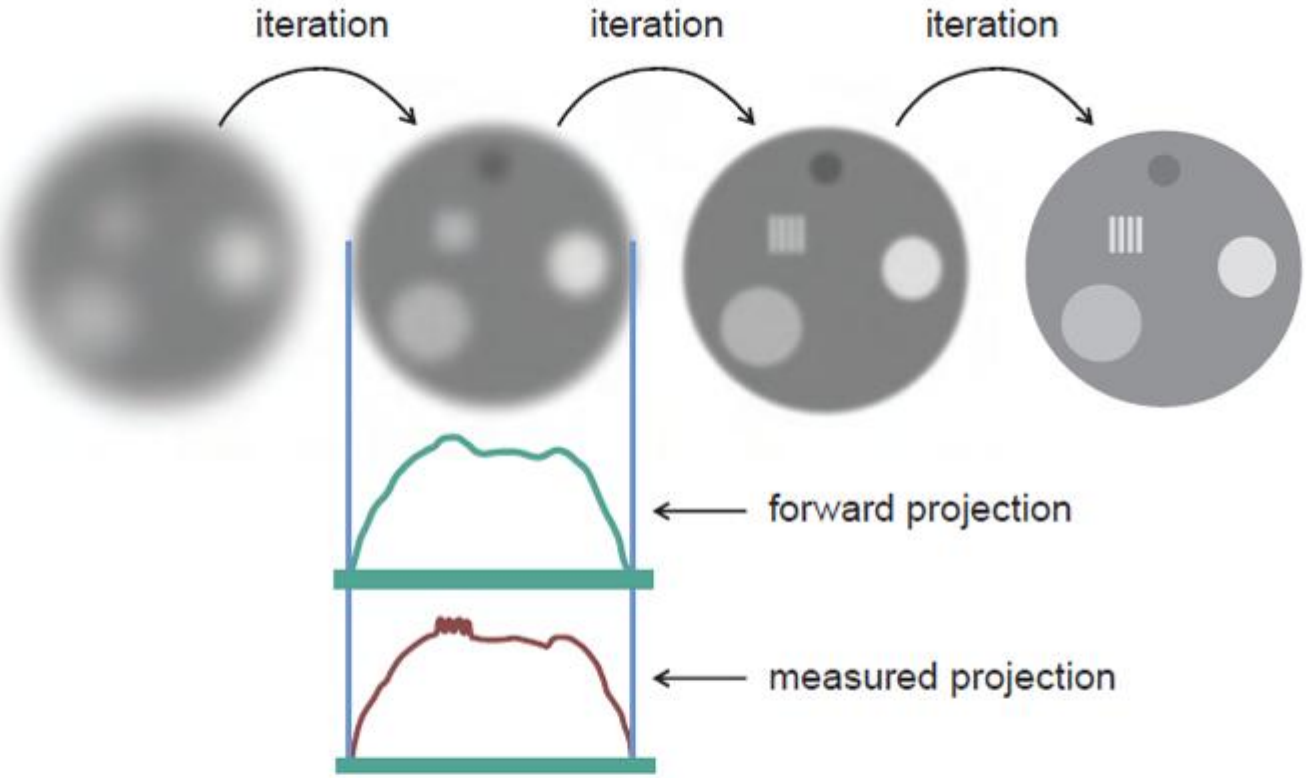

■ **FIGURE 10-55** The logic behind iterative CT image reconstruction is illustrated in this figure. The reconstruction process begins with an initial estimate of what the object may "look like." This guess is used to compute forward projection data sets, which are then compared with the measured projection data sets. The difference between the mathematical projections and the physical measurements creates an error matrix for each projection. Each type of iterative algorithm for reconstruction uses the error matrix and then updates the next iteration of the image. The process continues for a number of iterations until the error matrix is minimized, and the CT image at that point should be a good estimate of the actual object that was scanned.

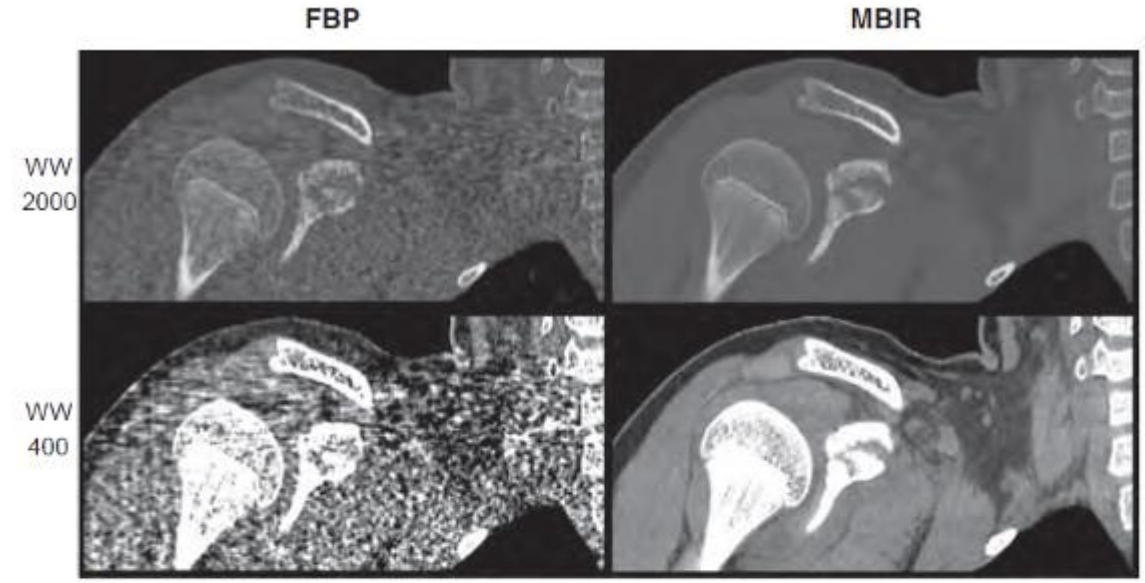

■ **FIGURE 10-56** Iterative reconstruction in CT is made possible by algorithms that are computationally efficient and require very few iterations. The iterative technique for reconstruction can in most cases extract more signal-to-noise ratio from the acquired data set, resulting in higher SNR reconstructed images compared to filtered backprojection techniques. Here, two images are illustrated showing the comparison from a clinical CT system, where the interactive reconstruction methods resulted in superior noise properties compared to filtered backprojection of the same acquired projection data. **A.** Filtered backprojection (FBP) is compared with model-based iterative reconstruction (MBIR) in this figure. **B.** This figure shows the same image produced by standard FBP, statistical iterative reconstruction, and model-based iterative reconstruction. (Courtesy J. Hsieh.)

ACR phantom –spatial resolution section

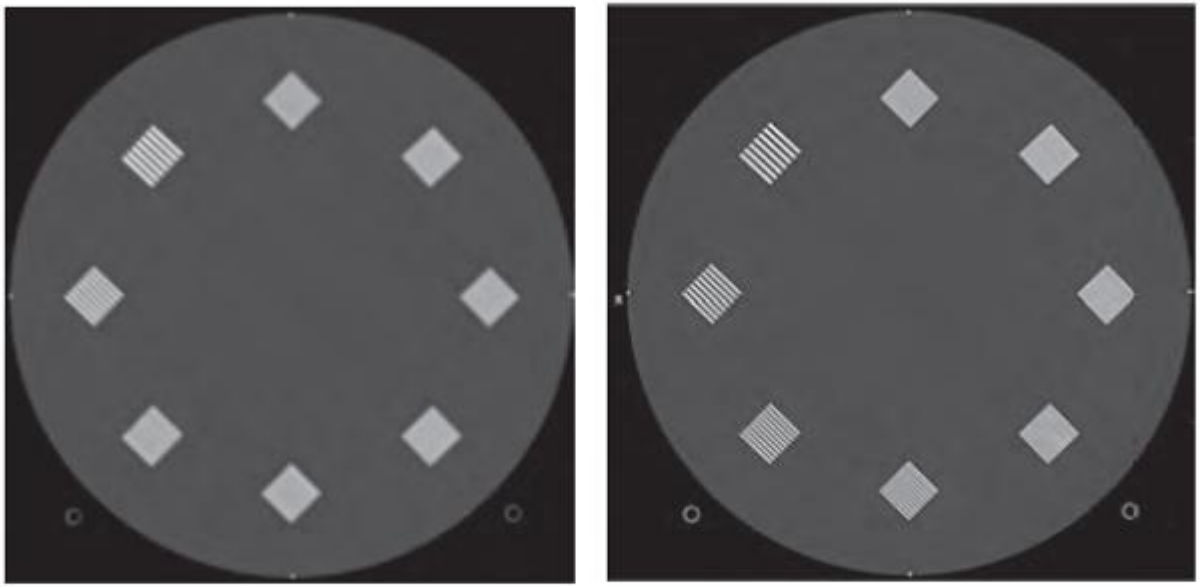

A. soft tissue kernel

B. bone kernel

■ **FIGURE 10-57** In the field measurements of spatial resolution in CT still rely on visual assessment of bar phantoms—in this figure, the resolution module from the American College of Radiology (ACR) CT accreditation phantom is shown, imaged with (**A**) a soft tissue reconstruction filter and (**B**) with a bone filter. The same CT acquisition can produce different images depending on which reconstruction filters are used.

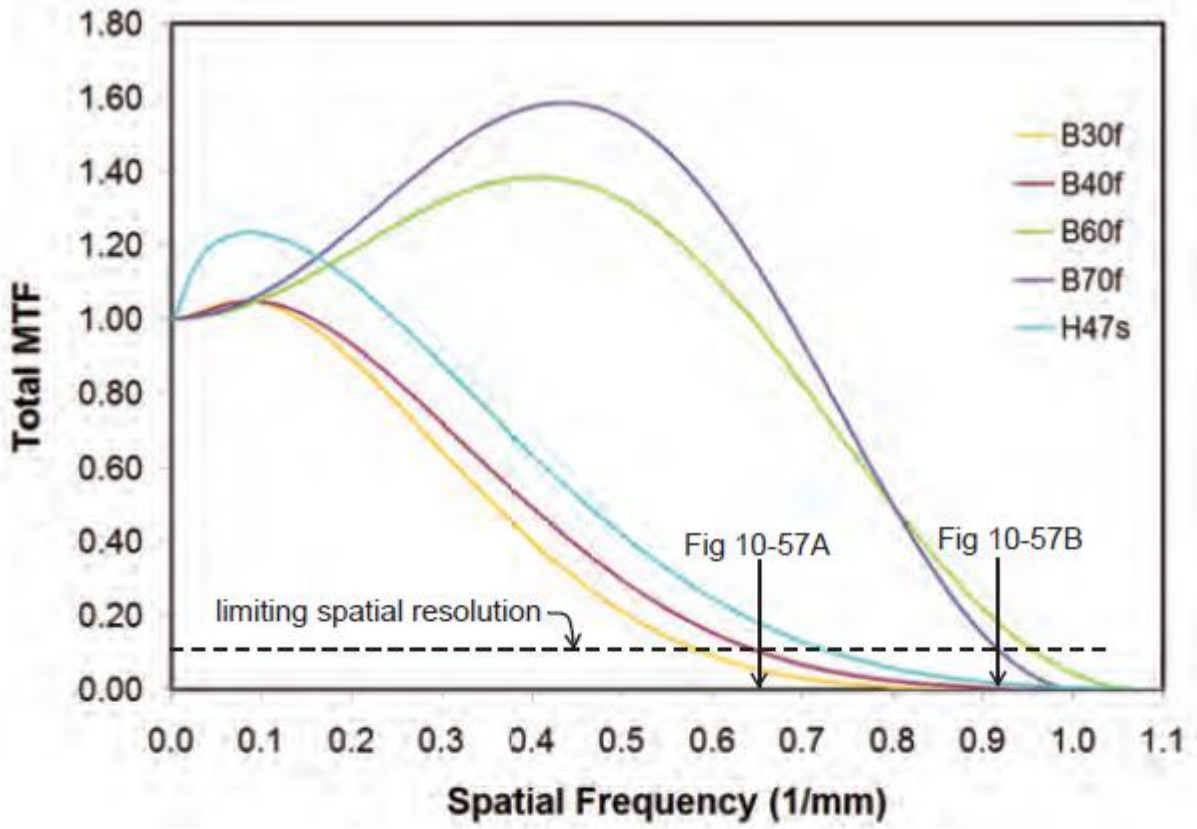

■ **FIGURE 10-58** Scientific evaluation of the resolution of CT images relies on the assessment of the modulation transfer function (MTF), as shown in this figure. This figure shows the dramatic impact on the MTF that various reconstruction filters have. (Courtesy K. Krzymyk.)

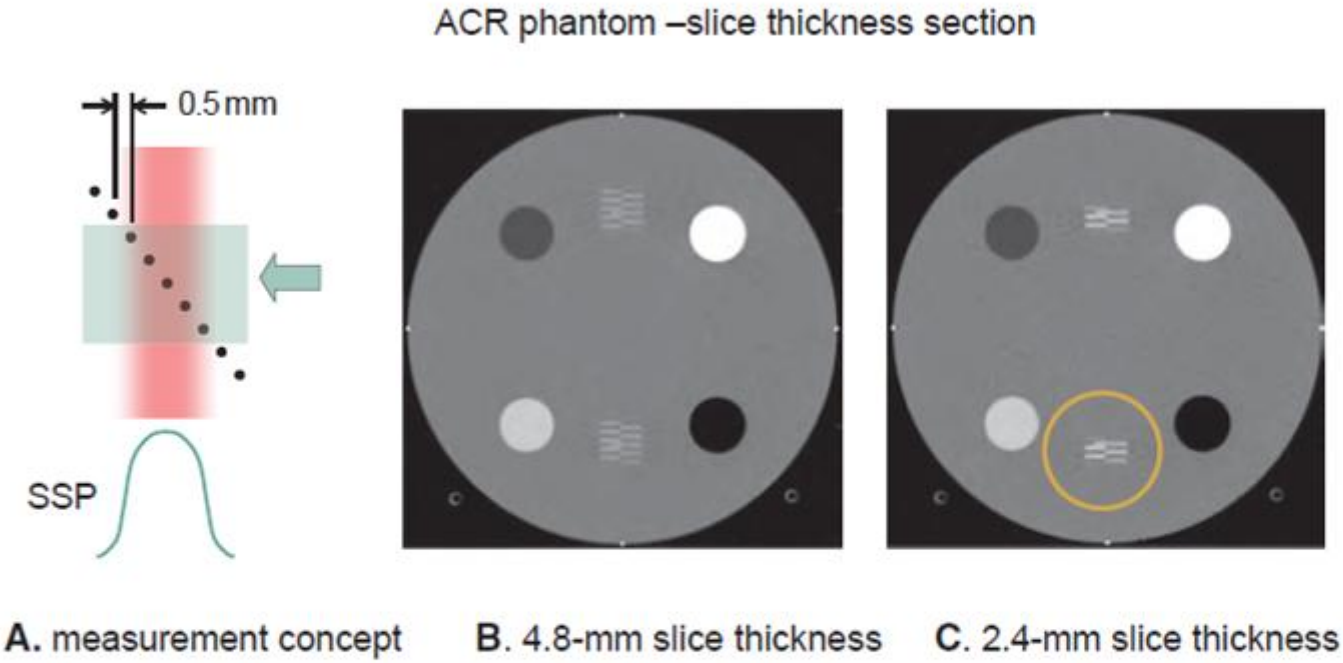

■ FIGURE 10-59 The spatial resolution in the z-dimension of the CT image has been traditionally measured by the slice sensitivity profile, SSP. The ACR phantom has a series of small wires positioned at 0.5-mm intervals along the z-axis of the phantom (**A**). After scanning the phantom, the number of visible wires is counted and multiplied by 0.5 mm, to estimate slice thickness. **B.** A 4.8-mm nominal CT scan of the ACR phantom is showed, and 10 wires are visible suggesting that the slice thickness is approximately 5.0 mm. **C.** A 2.4-mm nominal image through the ACR phantom is illustrated, with 6 wires visible suggesting a 3.0-mm measured slice thickness.

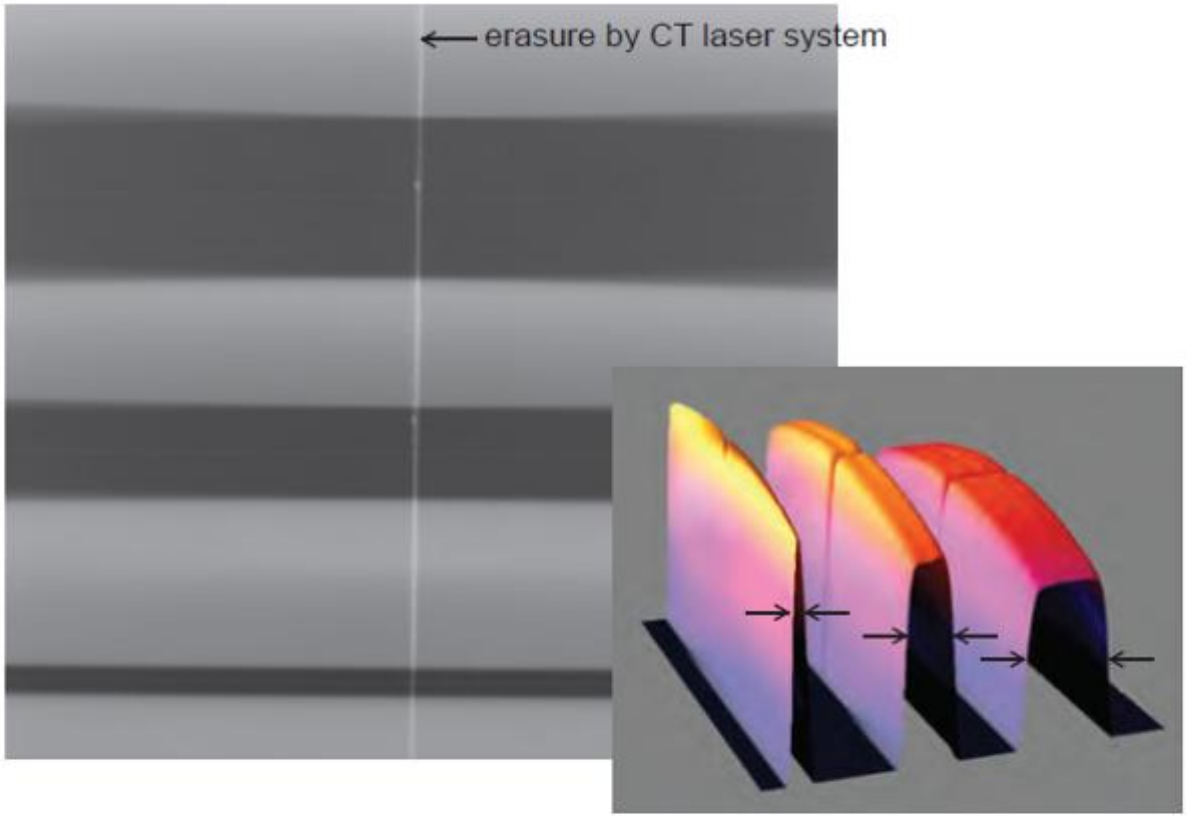

■ **FIGURE 10-61** The slice sensitivity profile, its discrete implementation in the ACR phantom, and the z-axis MTF all are measures of the z-axis *image* resolution. However, the overall dose profile along the z-axis can only be measured using an external device such as film or a computed radiography (CR) plate, the latter of which was used to generate the image data shown here. Various nominal collimated slice thicknesses (as set on the CT console) were used to scan a CT plate taken out of the cassette; the CR plate was moved along z to sequentially measure the dose profiles for different nominal slice thicknesses. The image data from the CR plate are plotted as isometric plots on the inset image. These plots show the dose profile along z for several different collimation thicknesses.

- **Kvaliteta slike – općeniti pojam koji se primjenjuje na sve vrste slika (medicinske, fotografske, TV i sl.)**
- **‘Kvaliteta’: subjektivni doživljaj, ovisan o funkciji slike**

- **Radiologija- mjera kvalitete radiološke slike je *korisnost u postavljanju adekvatne dijagnoze***

- **objektivne mjere kvalitete CT slika**

- **Atenuacija** je odstranjenje fotona iz snopa rtg zraka ili gama zraka prilikom prolaska kroz materiju.
- **Linearni atenuacijski kojeficijent (LAK)** je broj koji opisuje razinu oslabljenja intenziteta energije snopa tijekom prolaska kroz sloj određene tvari.
- Linearni atenuacijski kojeficijent označava se **μ**, i mjeri se cm^{-1}
- Mali **μ** označava da je materijal relativno transparentan (npr. meko tkivo ili zrak), dok veliki **μ** pokazuje veći stupanj gustoće (npr. kost)
- Linearni atenuacijski kojeficijent je ovisan o vrsti materijala i energiji zračenja.
- Izmjereni intenzitet ***N*** „transmitiran" kroz sloj tvari debljine ***x*** i gustoće **ρ** u odnosu na ulazni intenzitet N_o prikazan je jednadžbom

$$N = N_o e^{-\mu x}$$

Kontrast

- **Kontrast je posljedica razlike u gustoći između jediničnih segmenta slike (voxel/pixel)**
- **Kontrast u slici rezultat je brojnih različitih koraka koji se događaju tijekom nastanka,obrade i prikaza slike**

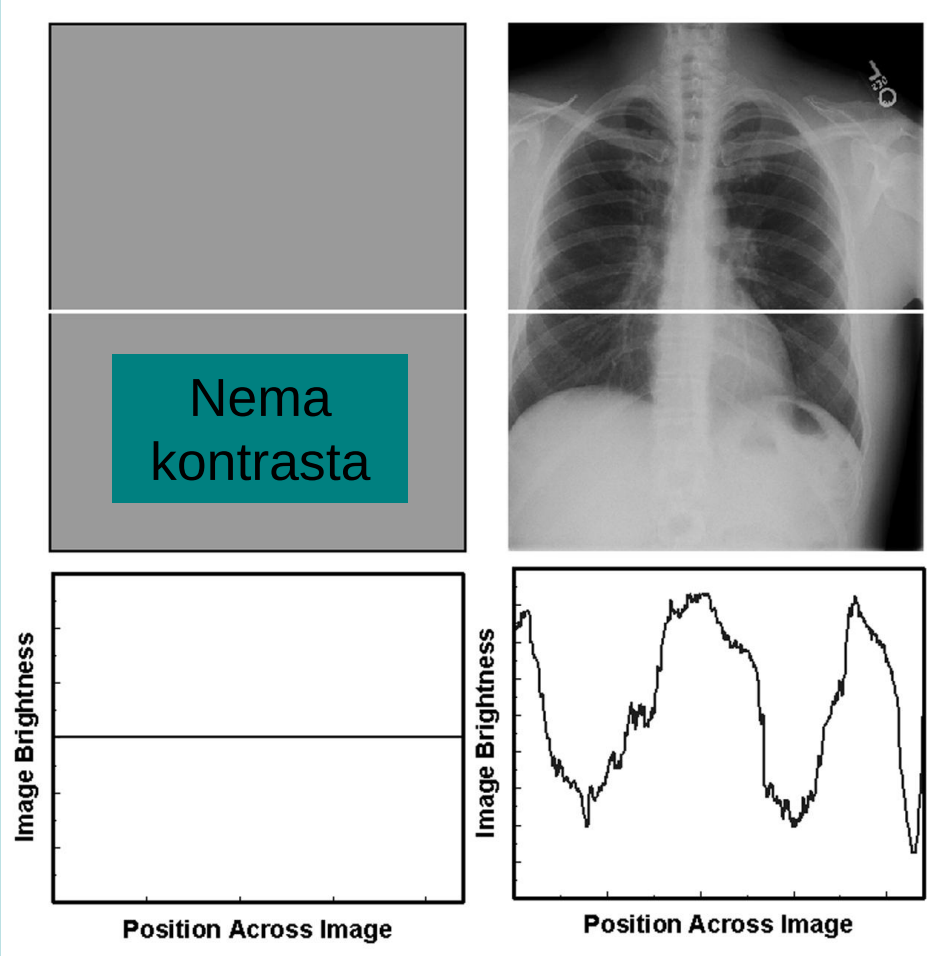

c.f. Bushberg, et al. The Essential Physics of Medical Imaging, 2nd ed., p. 256.

Kontrast

- Ako je snop x-zraka usmjeren na homogeni materijal različite debljine onda će broj „transmitiranih” x-zraka kroz tanki dio biti veći nego kroz deblji dio.

- **Kontrast ovisi o razlici u debljini**

- **C = (A-B)/A,** Budući je A<B, C će biti broj između 0.0 - 1.0
- Za $A=N_0e^{-\mu x}$ and $B=N_0e^{-\mu(x+z)}$
- $C = 1-e^{-\mu z}$
- Gdje je μ atenuacija, a **z** je debljina
- Kada je z=0, $e^{-\mu z} = 1$, C = 0

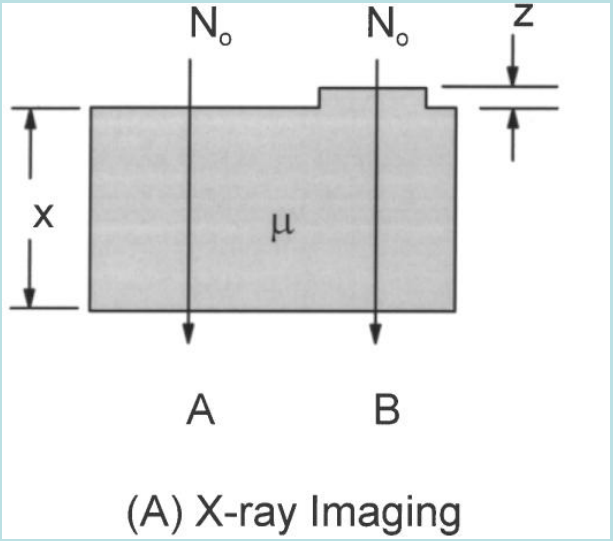

(A) X-ray Imaging

c.f. Bushberg, et al. The Essential Physics of Medical Imaging, 2nd ed., pp. 257-258.

ontrast

- $C = 1-e^{-\mu z}$
- Ako se z povećava, tada se i C povećava
- Ako se μ povećava, tad se i C povećava
- μ se povećava kada se energija of x-snopa smanjuje

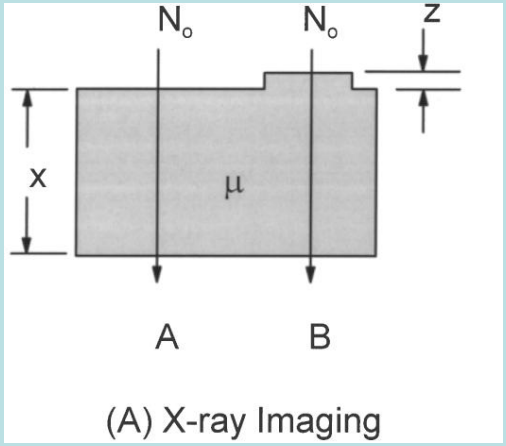

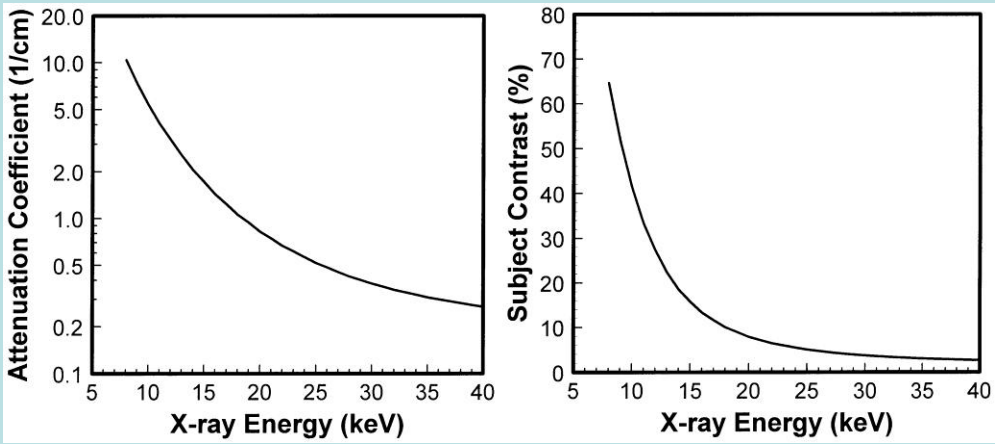

c.f. Bushberg, et al. The Essential Physics of Medical Imaging, 2nd ed., pp. 257-258.

© UW and Kalpana M. Kanal, Ph.D., DABR

Detektor Kontrast (Film)

- **Karakteristike detektora igraju vrlo važnu ulogu u nastanku kontrasta na završnoj slici**
- **Kontrast je u principu određen time kako detektorska 'mapa' prenosi energiju na izlazni siganal**
- **Primjer: Karakteristična krivulja (e.g., H&D curve)**
- **Radiografski kontrast ΔOD**

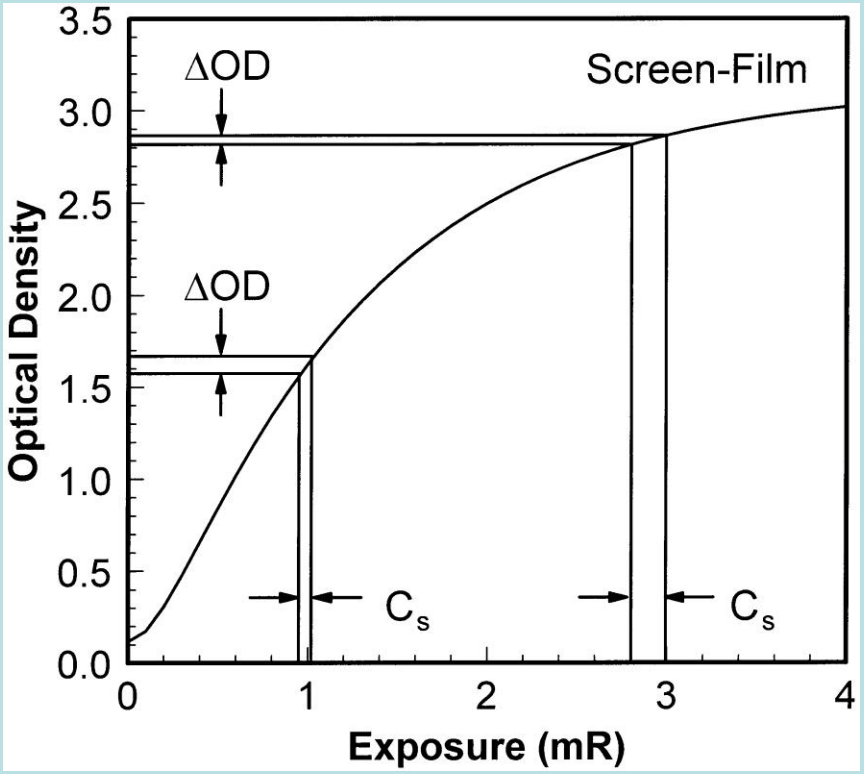

c.f. Bushberg, et al. The Essential Physics of Medical Imaging, 2nd ed., p. 260.

© UW and Kalpana M. Kanal, Ph.D., DABR

Detektor/Monitor / (Film) Kontrast

- Za monitor-film radiografiju i mamografiju, radiografski kontrast , C je:
- $C = OD_A - OD_B$, A i B su susjedne regije na rtg. slici
- U radiografiji kontrast općenito nemože biti poboljšan ili promjenjen na rtg. filmu
- Relativna svjetlina slike (ovisna o kontrastu) kao funkcija debljine pacijenta je ovisna o kontrstnosti objekta, detektorskom kontrastu i prosječnoj svjetlini negatoskopa

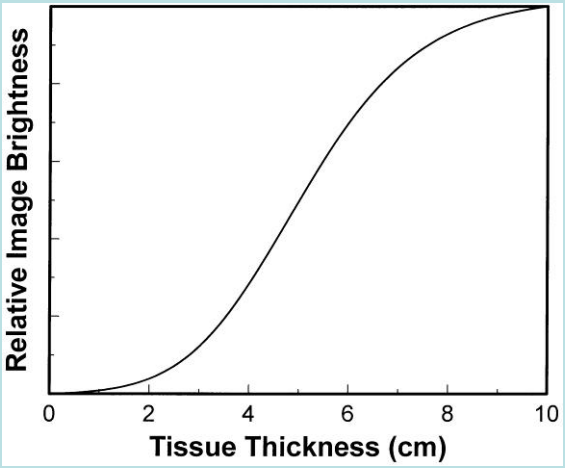

c.f. Bushberg, et al. The Essential Physics of Medical Imaging, 2nd ed., pp. 261.

Kontrasnost digitalne slike (Contrast-to-Noise Ratio)

- Kada imamo digitalnu sliku, serija “postprocesing” koraka se automatski izvodi na slici
- Uobičajeni processing je subtrakcija od konstantnog broja (recimo, k) od slike.
- Kontrast = [(A-k)-(B-k)] / (A-k)

  = (A-B) / (A-k)
- Ako je k = A/2, kontrast je dvostruko povećan, ako je k = A, contrast je nepromjenjen, k = negativan, kontrast je smanjen
- U ovisnosti o izabranom k, kontrast može biti radikalno promjenjen

Kontrasnost digitalne slike (Contrast-to-Noise Ratio)

- Korisnija mjera kontrasnosti digitalne slike je pojam
- “contrast-to-noise ratio”, CNR

- **CNR = (A-B)/σ, with σ = šum slike**

- Zbog mogućnosti post-process digitalne slike, CNR je znatno relevantniji pojam

Prikaz Kontrastnosti (Digitalna Slika)

- Glavna prednost digitalne slike je
- da prikazana kontrastnost može
- biti promjenjena u realnom
- vremenu

- Vrijednost sive-skale je
- konvertirana u svjetlinu na
- monitoru korištenjem
- “look-up table” (window and level)
- nagib “look-up table” je povezan
- sa prikazom kontrasnosti na slici

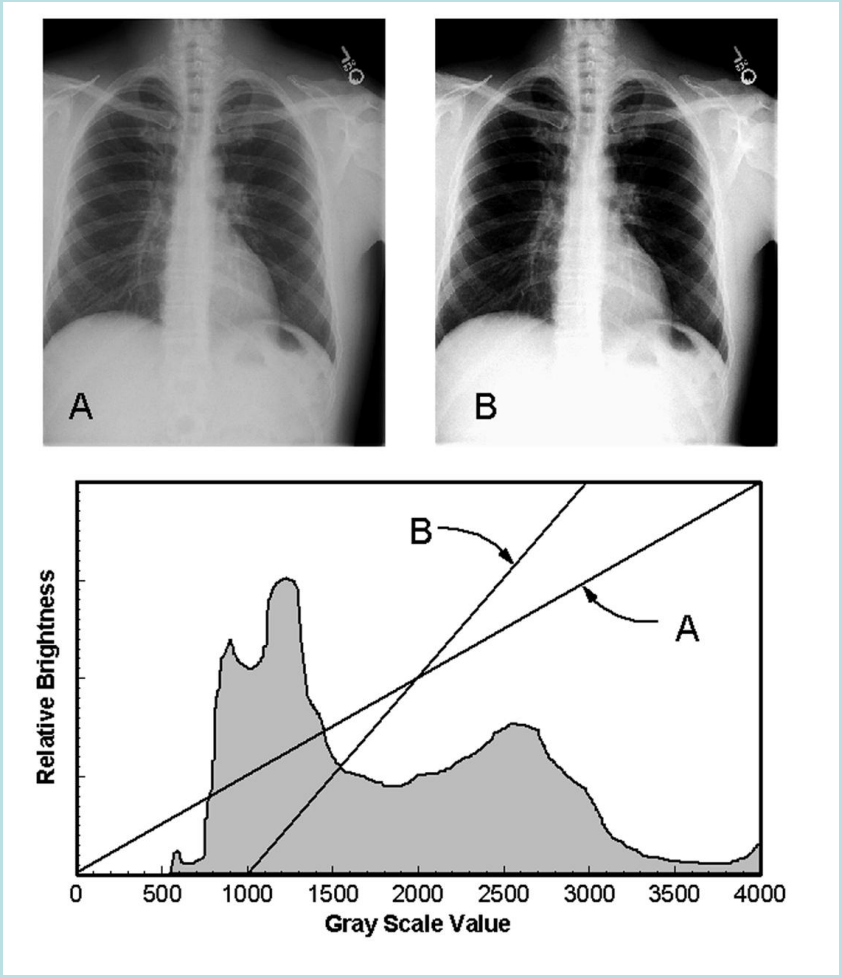

c.f. Bushberg, et al. The Essential Physics of Medical Imaging, 2nd ed., p. 262.

- Prostorna rezolucija je sposobnost “imaging systema”
- da razluči (prikaže) dva susjedna “high-contrast” objekta kao odvojene entitete
- 2D &3D: x, y (visina i širina (mm)) i siva skala & digitalna vrijednost
  - Što je više piksela, bolja je rezolucija.

Bolja rezolucija

- Prostorna rezolucija može se opisati terminom “high-contrast resolution”,
- zamućenje
- “modulation transfer function” (MTF)
- Može se izraziti brojem parova linija po milimetru (lp/mm)
  - Par linija uključuje opacificirani i prozračni dio

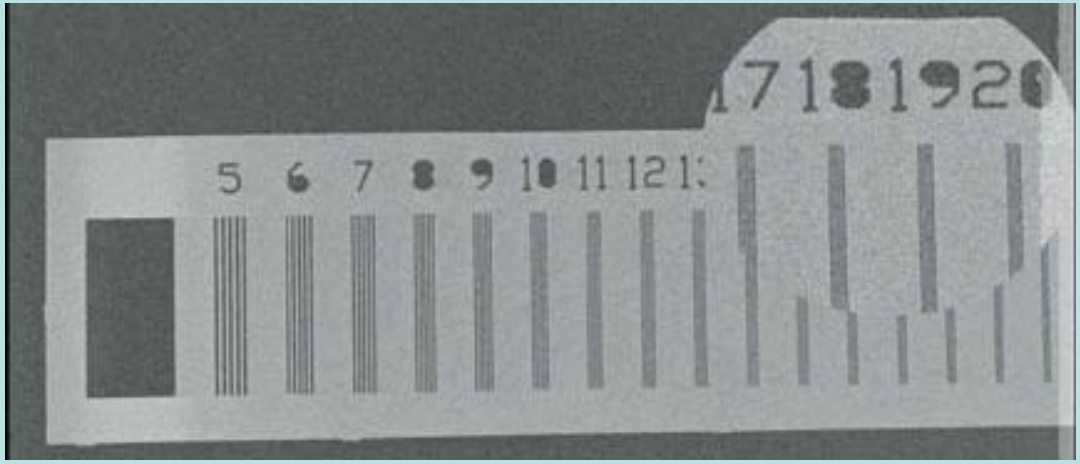

Fizikalni mehanizmi “zamućenja”

- Zamućenje je posljedica niza faktora
- Zamućenje utječe na prostornu rezoluciju
  - Optička difuzija (monitor pojačala)
  - Micanje (nevoljno, pulsacija)
  - Debljina sloja (kut nagiba) u tomografiji
  - Žarišna točka zamućenje i povećanje slike

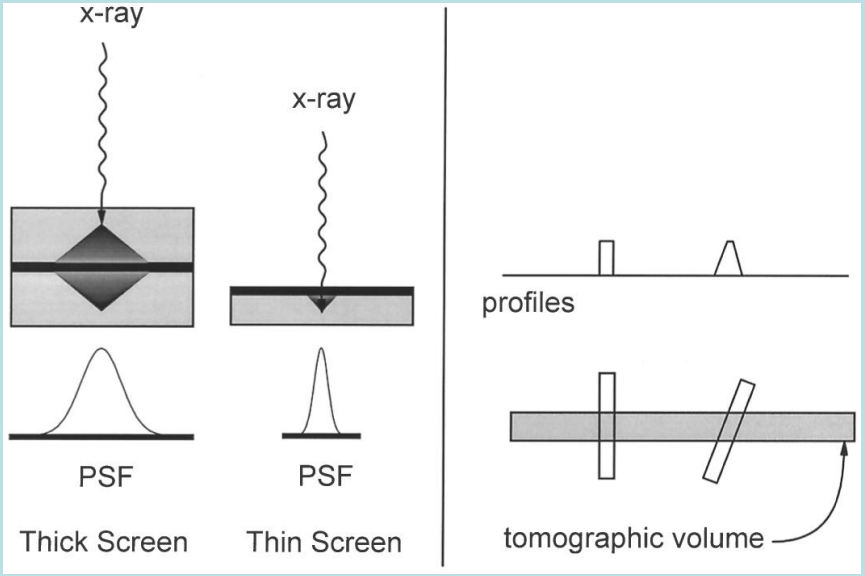

c.f. Bushberg, et al. The Essential Physics of Medical Imaging, 2nd ed., pp. 266.

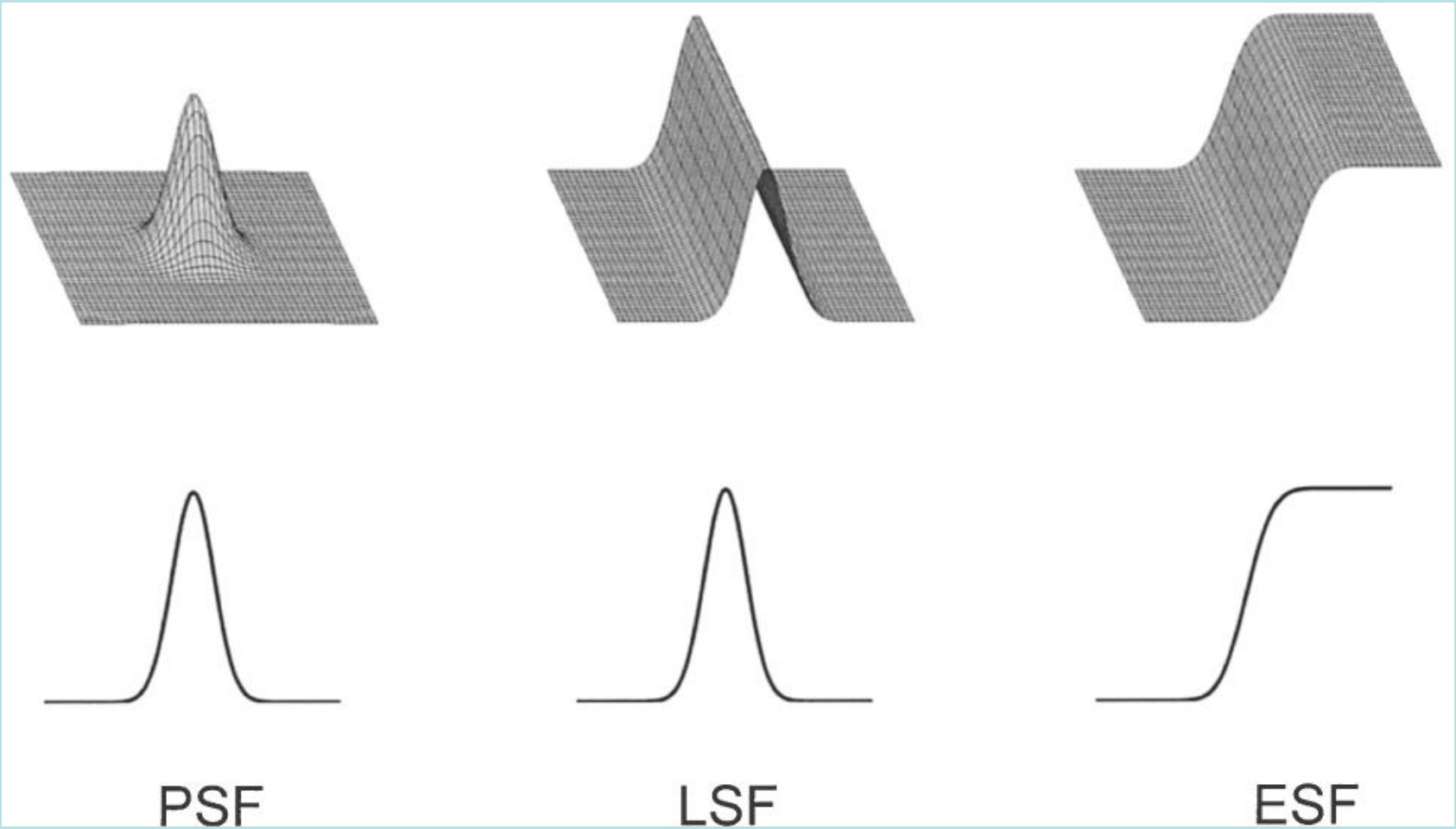
PSF
LSF
ESF

Prostorna domena: Point Spread Function

- **Metoda mjerenja prostorne rezolucije:**
  - **točkasti stimulus detektorskog sistema**

- **Nastala slika je "point response function" ili "point-spread function" (PSF)**
- **Stupanj „zamućenja" (blurring) točke je mjera kvalitete „imaging sistema"**

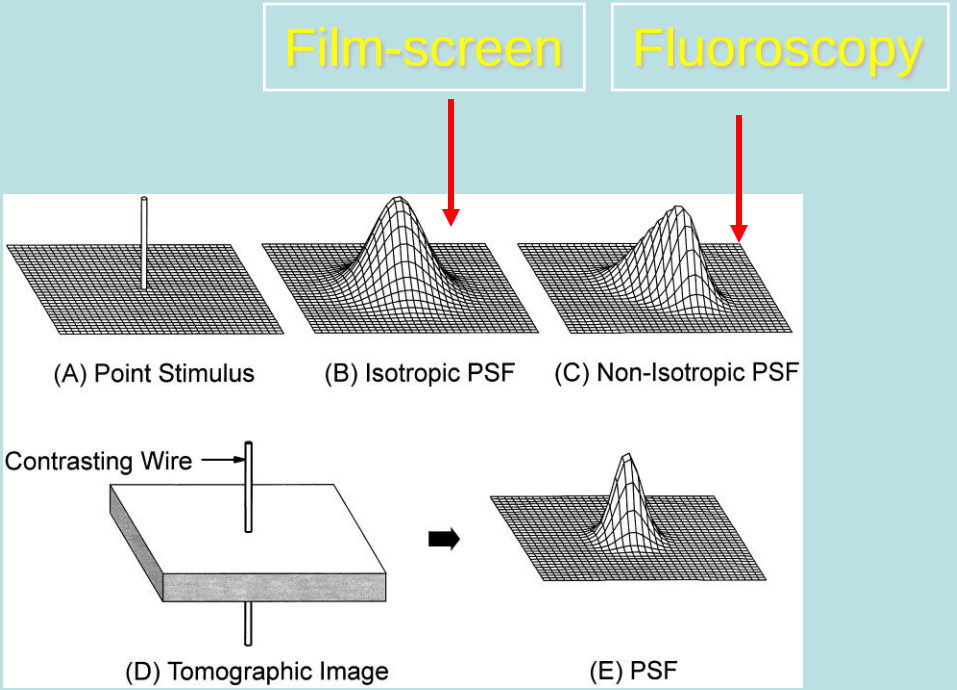

c.f. Bushberg, et al. The Essential Physics of Medical Imaging, 2nd ed., p. 264.

LSF i ESF (mjere zamućenja)

- Line spread function (LSF) koristi linearnu pukotinu za opisivanje
- odgovora imaging sistema na linearni stimulus
  - koristi se kod fluoroskopskoih sustava
- Možemo je zamisliti kao nakupinu velikog broja točkastih stimulusa
- Edge spread function (ESF) koristi glatki rub (kada je potrebno veliko područje ekspozicije) umjesto točkastog ili linijskog stimulusa, korisna mjera za raspršno zračenje

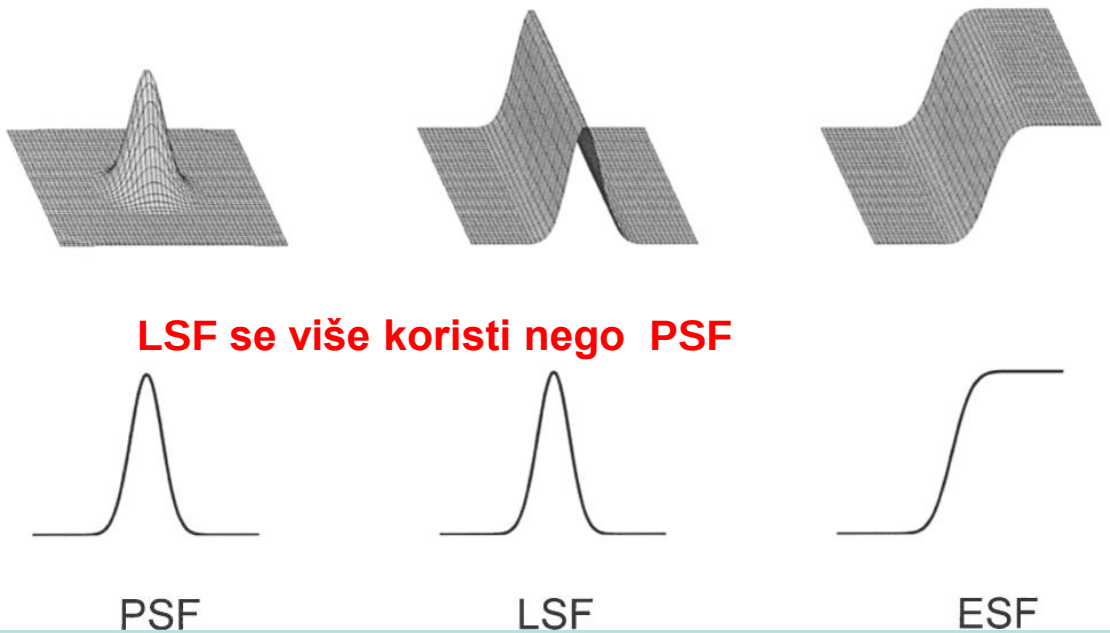

c.f. http://www.sprawls.org/resources/BLUR/classroom.htm

a. Line Spread Function (LSF)

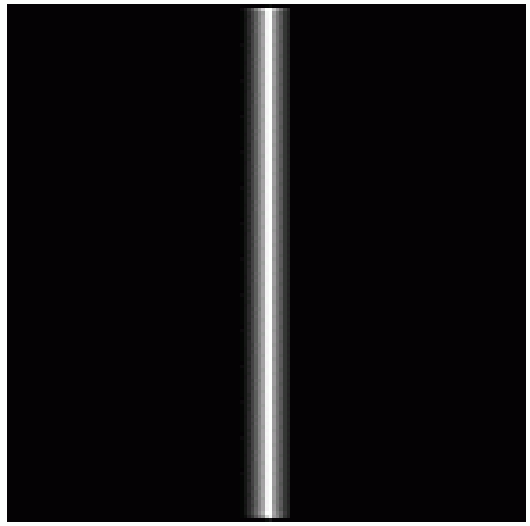

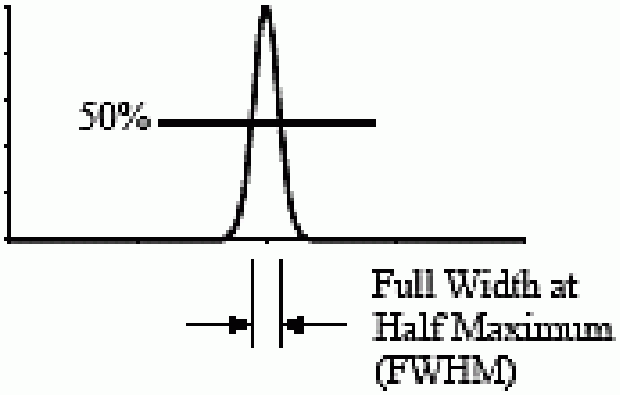

http://www.dspguide.com/graphics/F_25_3.gif

- Zvučni val: f (cycles/sec) = 1/T (sec)
- Prostorna frekvencija
  - **F = ½ Δ**
  - Gdje je Δ veličina objekta u mm
  - ciklus/mm ili par linija/mm
- Niska prostorna frekvencija → veći objekt u slici
- Viska prostorna rezolucija → manji objekti
- Jednostavno prostorna rezolucija je drugačiji način
- razmišljanja o veličini objekta
- 0.05 mm → 10 lp/mm
- 0.25 mm → 2 lp/mm

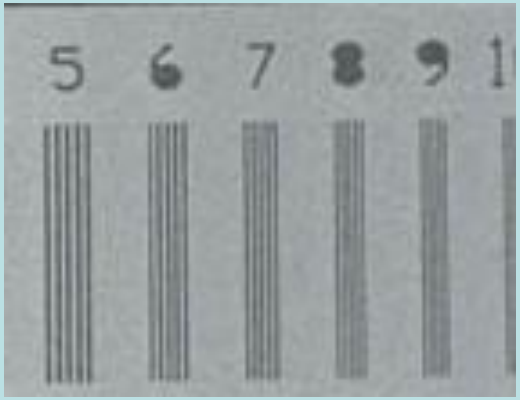

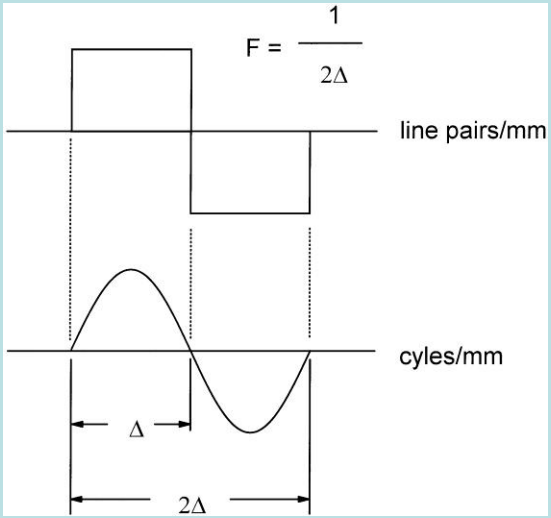

c.f. Bushberg, et al. The Essential Physics of Medical Imaging, 2nd ed., p. 269.

Modulation Transfer Function: MTF(f)

- “Modulation transfer function”, MTF je karakterizacija imaging sistema temeljem prostorne frekvencije
- MTF prikazuje udio ili postotak kontrasta objekta koja je zabilježena imaging sistemom, kao funkcija veličine (i.e., prostorna frekvencija) objekta
- MTF se može opisati načinom reakcije imaging sistema u ovisnosti o veličini stimulusa

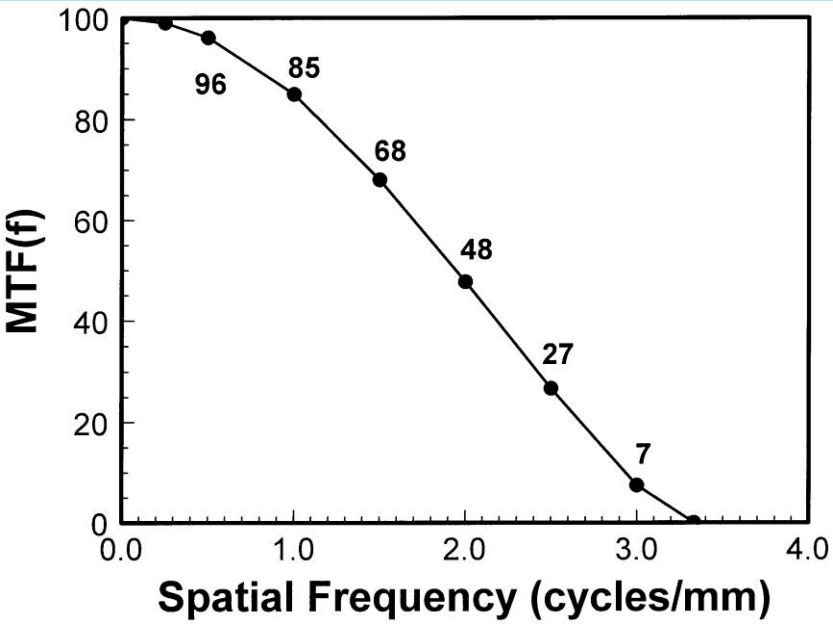

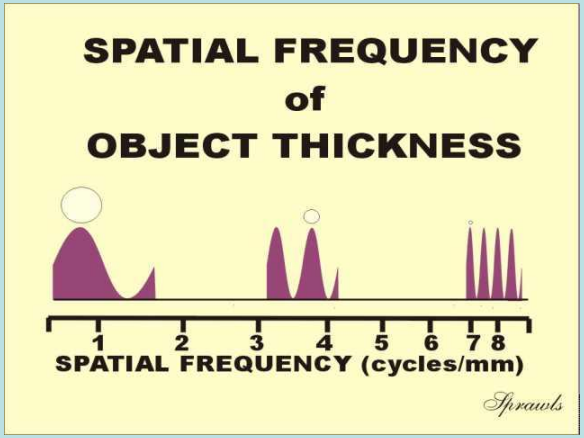

c.f. Bushberg, et al. The Essential Physics of Medical Imaging, 2nd ed., pp. 270-271.

MTF(f) „Imaging" Sustava

- Imaging chains:
  - ✓ $MTF_{system} = A \times B \times C$
  - ✓

Najslabija karika – dio sustava s najgorim MTF često određuje cijeli sistem "

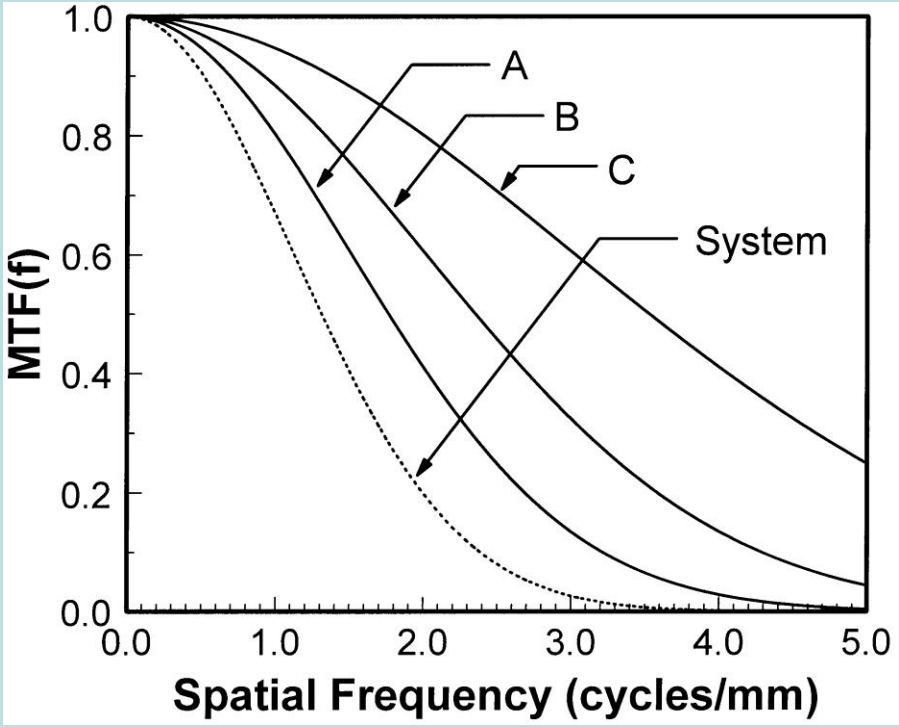

c.f. Bushberg, et al. The Essential Physics of Medical Imaging, 2nd ed., p. 272.

© UW and Kalpana M. Kanal, Ph.D., DABR

Kako prelazimo iz prostorne domene u frekventnu domenu

- **MTF(f) = |FT{LSF(x)}|**

Fourier transformacija, FT je integralna matematička operacija koja konvertira prostornu domenu (x) signala u funkciju prostorne frekvencije

(f) LSF (širi) ↑ MTF ⟶ 0

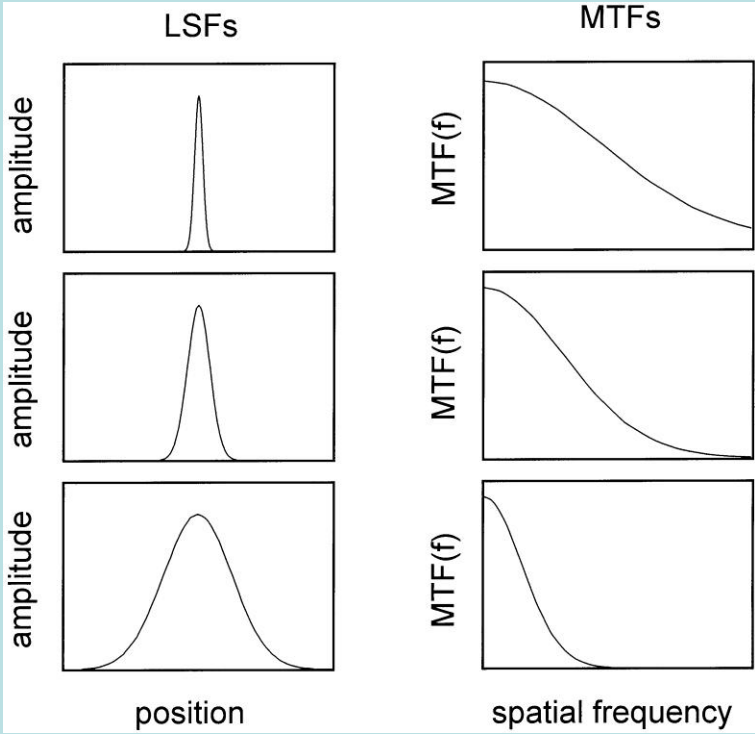

c.f. Bushberg, et al. The Essential Physics of Medical Imaging, 2nd ed., pp. 272-273.

$$\sigma = \sqrt{\frac{\sum_{i=1}^{N}\left(HU_i - \overline{HU}\right)^2}{N-1}} \qquad [10\text{-}12]$$

ACR phantom – low contrast detectability section

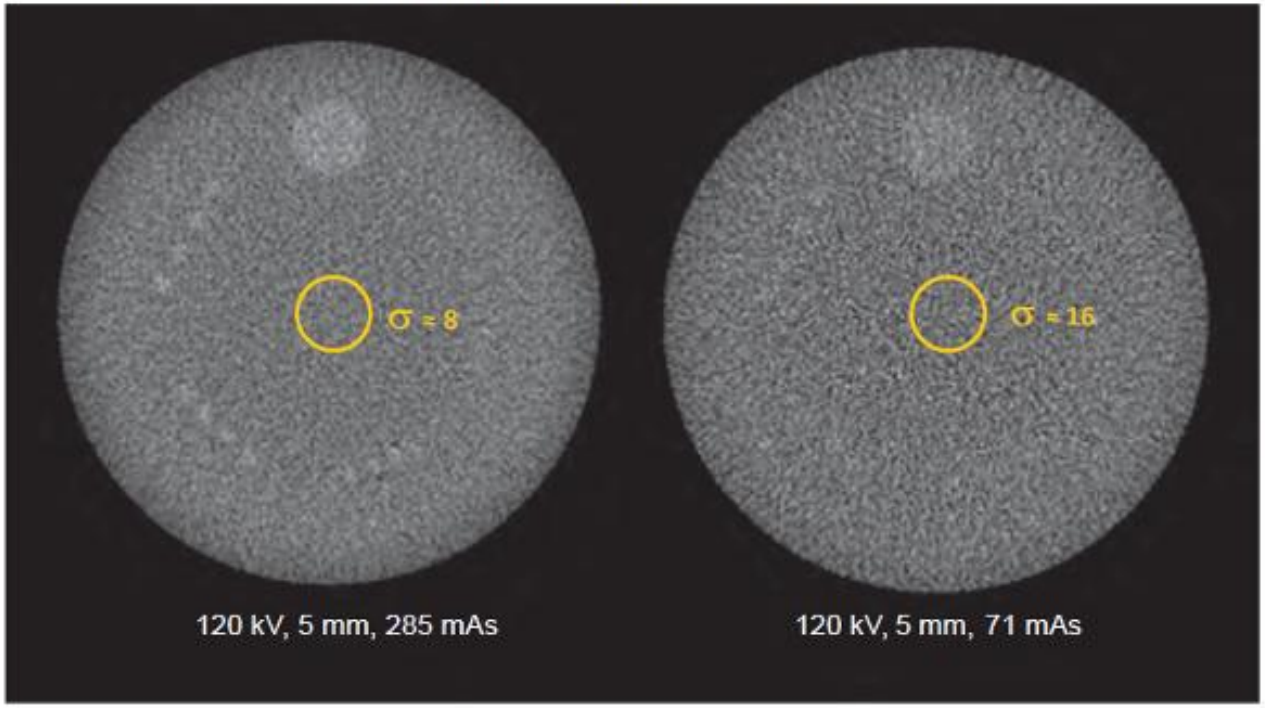

■ **FIGURE 10-62** CT images of the low-contrast module of the ACR phantom are illustrated, for radiation dose levels varying by about a factor of 4 (285 mAs/71 mAs ≈ 4.0). The circles visible in the phantom correspond to 0.6% differences in contrast (6 HU), and different rows of the circles have different diameters, which result in different signal-to-noise ratios (SNRs) of the circles. It is clear that more of the circular test objects are visible in the higher dose image on the left. The standard deviation, σ, is measured using software on most CT scanners or PACS systems. The standard deviation is seen to vary by a factor of two, for these images that used a fourfold difference in radiation dose, illustrating the Poisson relationship that image noise is relative to the square root of the dose.

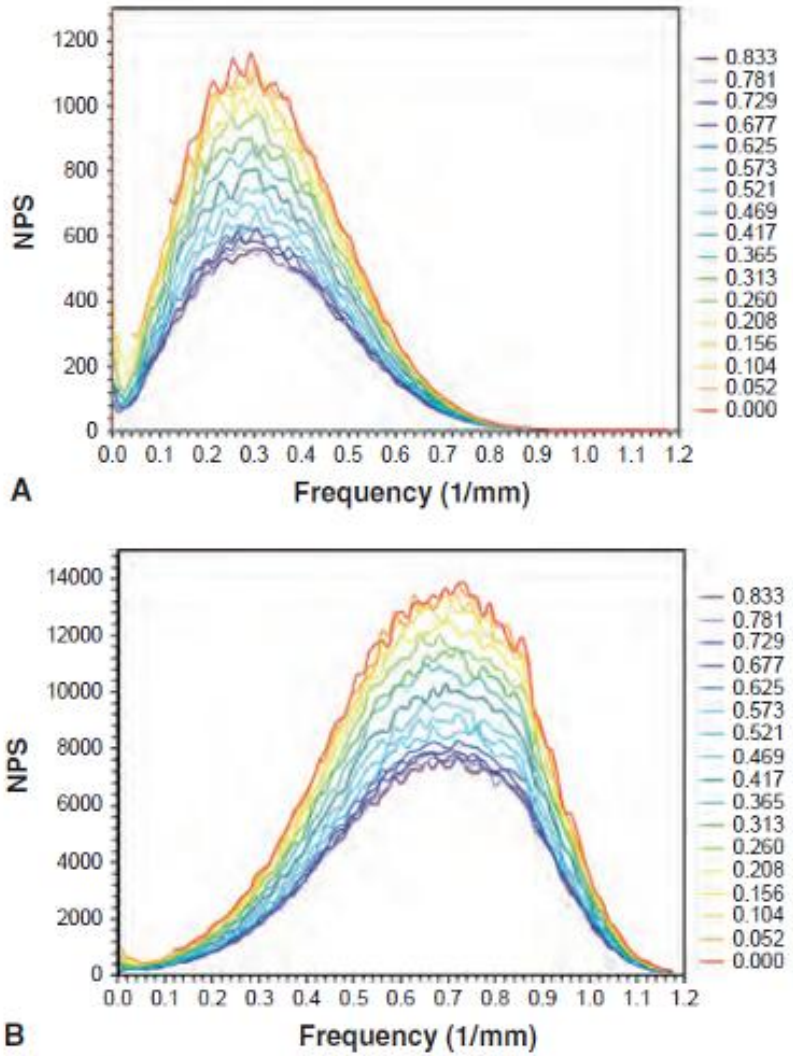

■ **FIGURE 10-63** The three-dimensional noise power spectra (NPS) are illustrated for (**A**) a standard body kernel. These data were computed computing the 3D Fourier transform from volumes of interest (VOIs) in a homogeneous region of a polyethylene phantom. The family of curves illustrates the z-axis dependency of the NPS, with the f_z values listed in the legend on the right. The figure on the right (**B**) illustrates similar data for the higher bandpass (bone) reconstruction kernel. (Courtesy SE McKenney.)

■ **FIGURE 10-66** Streak artifacts from high-density, high atomic number dental fillings are seen in this image. Streak artifacts are amplified in effect if there is slight motion of the high-density object. Patients' who move their jaw or swallow during a head CT can generate significant artifacts due to this.

Vodom ispunjeni cilindrični fantom
Isporučen sa uređajem
Koristiti za QC program

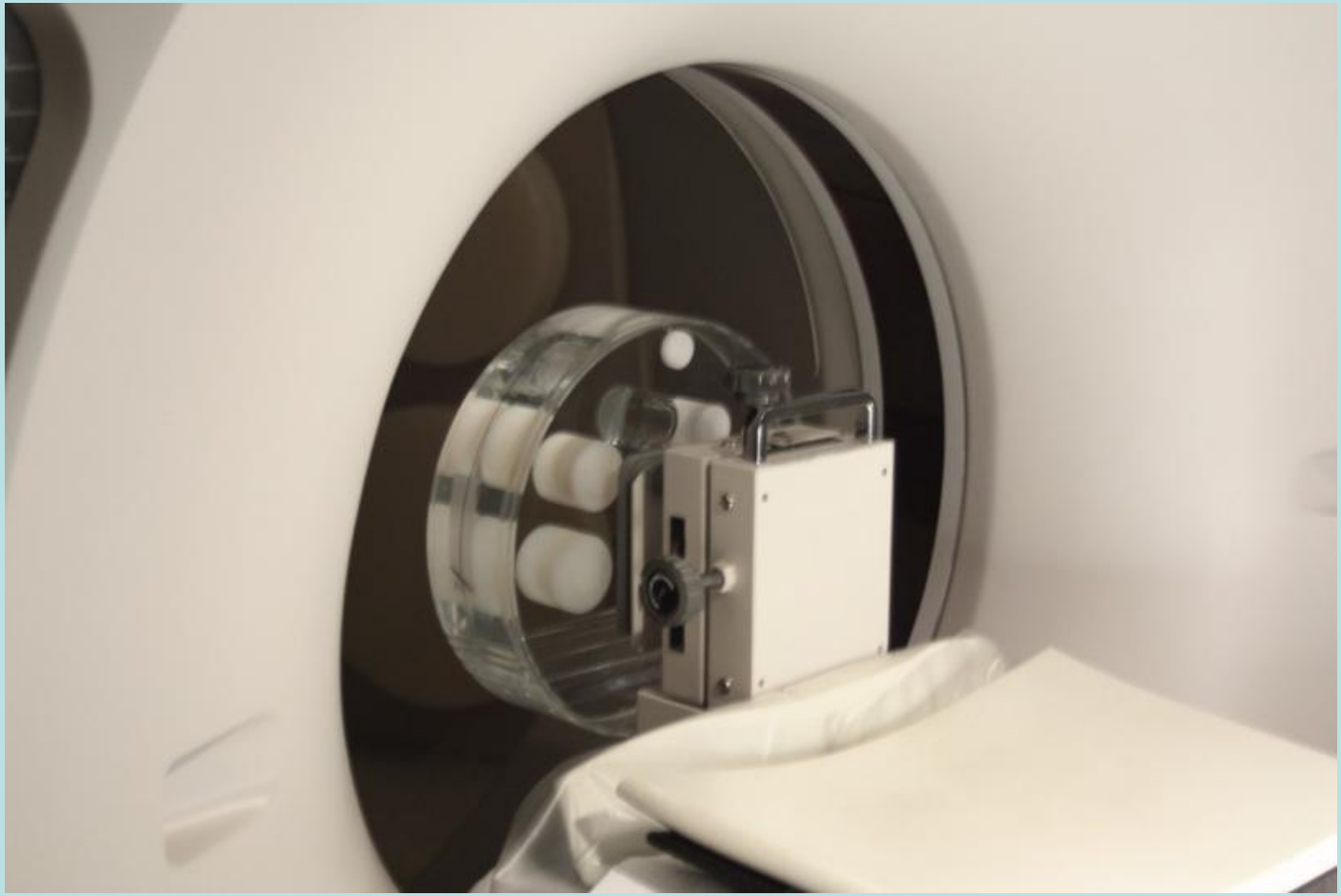

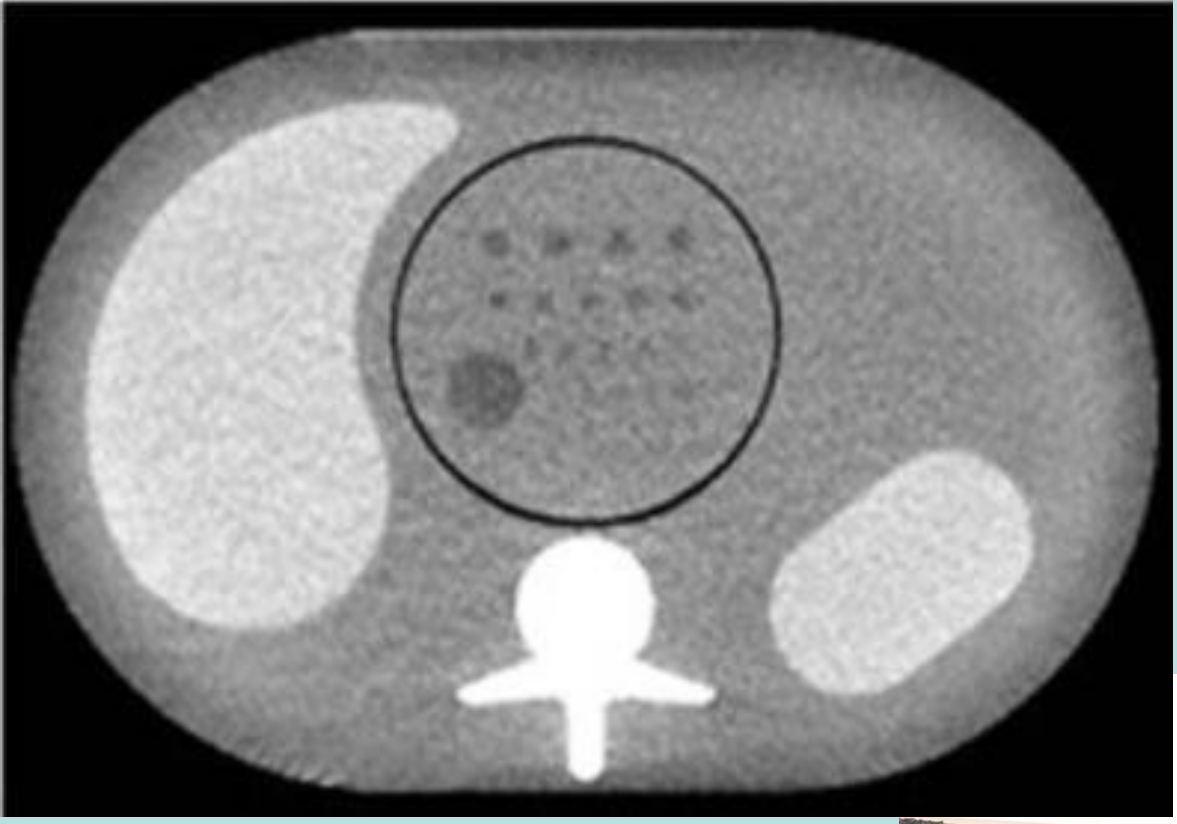

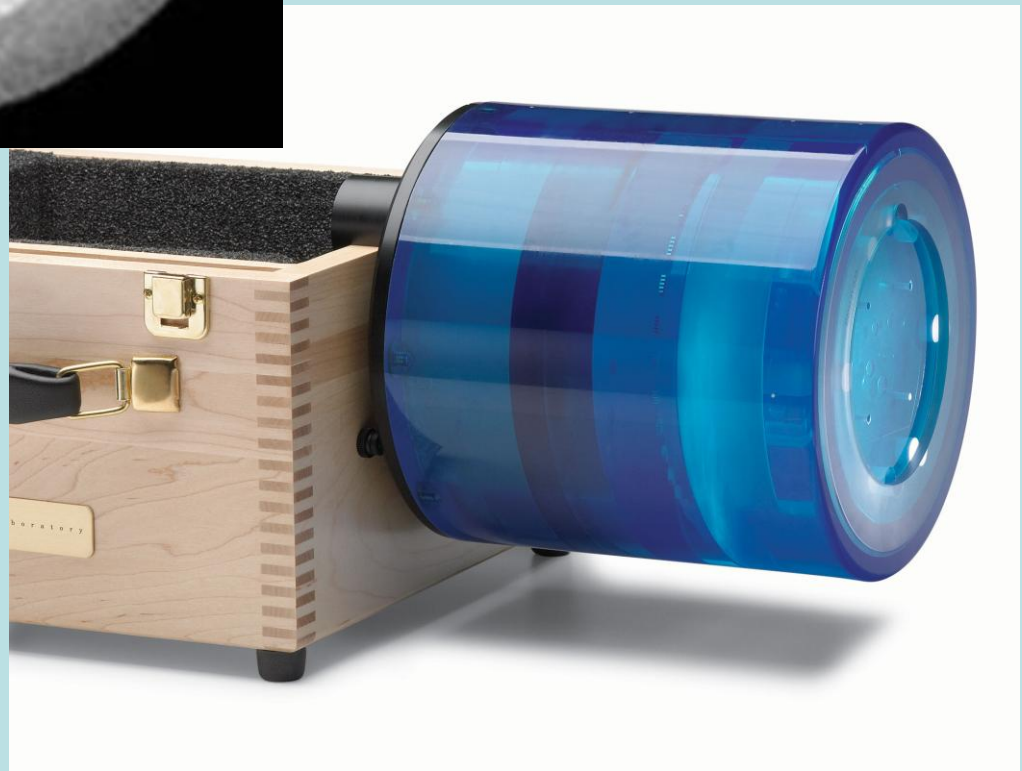

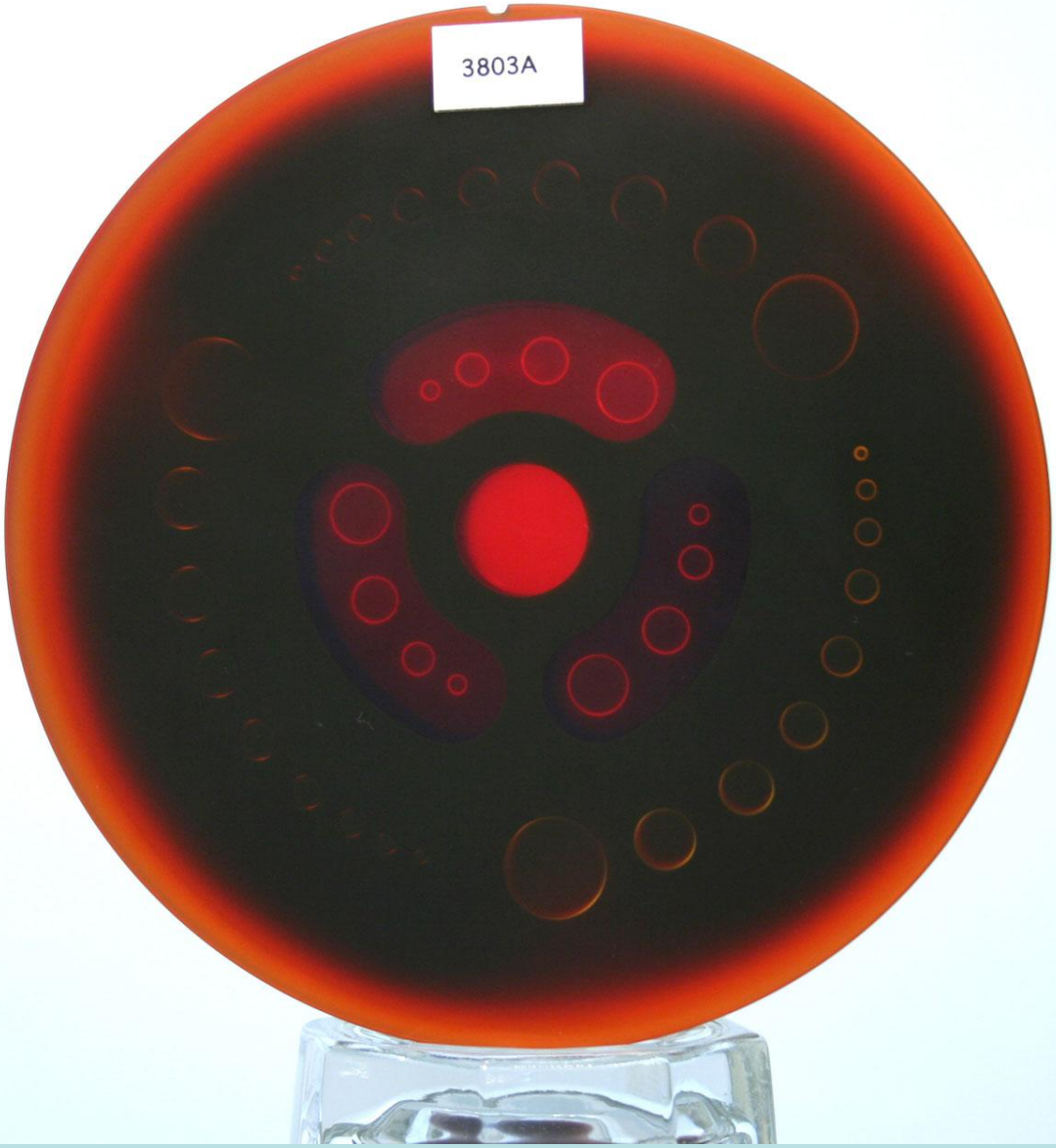
3803A

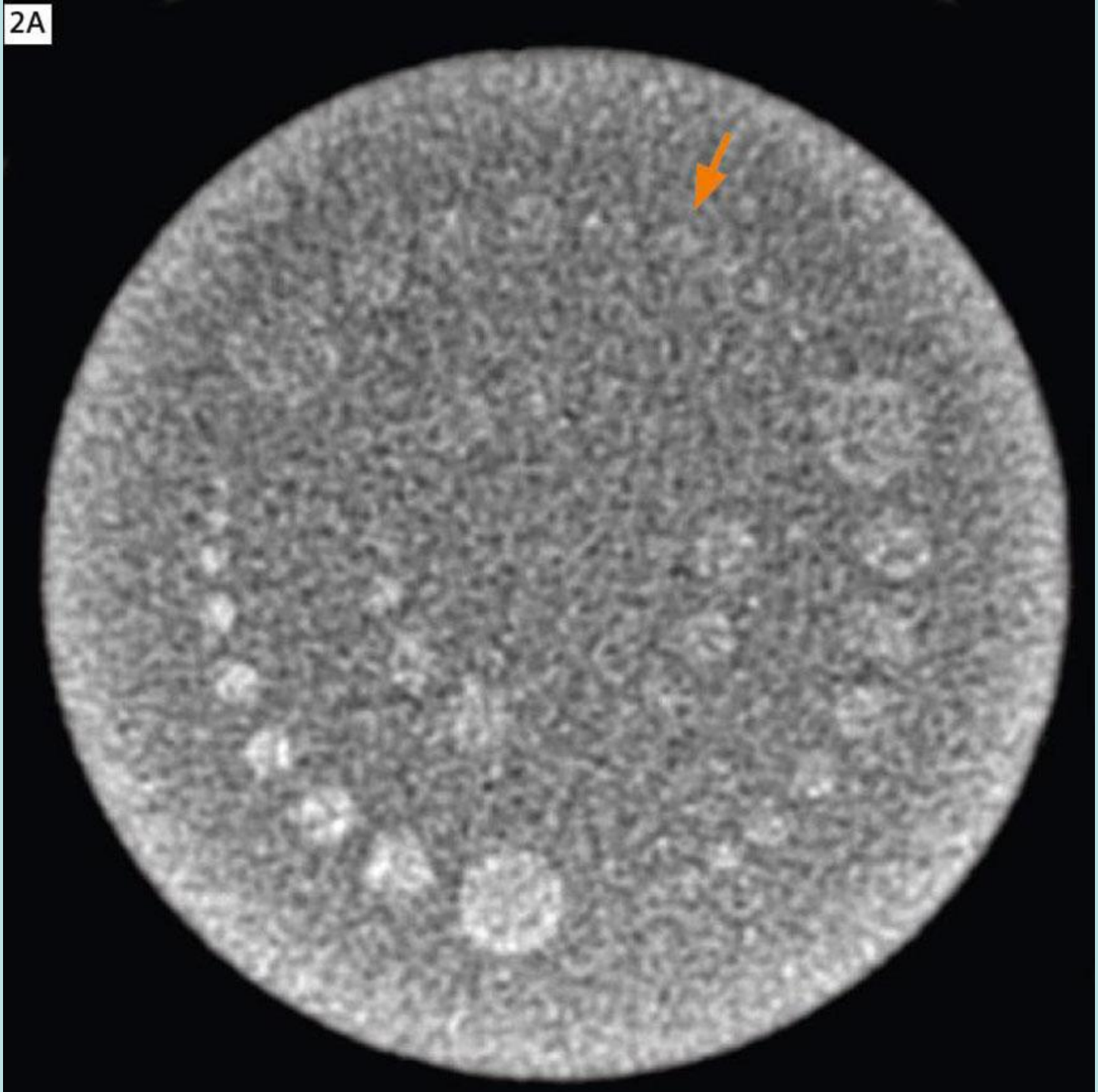
2A

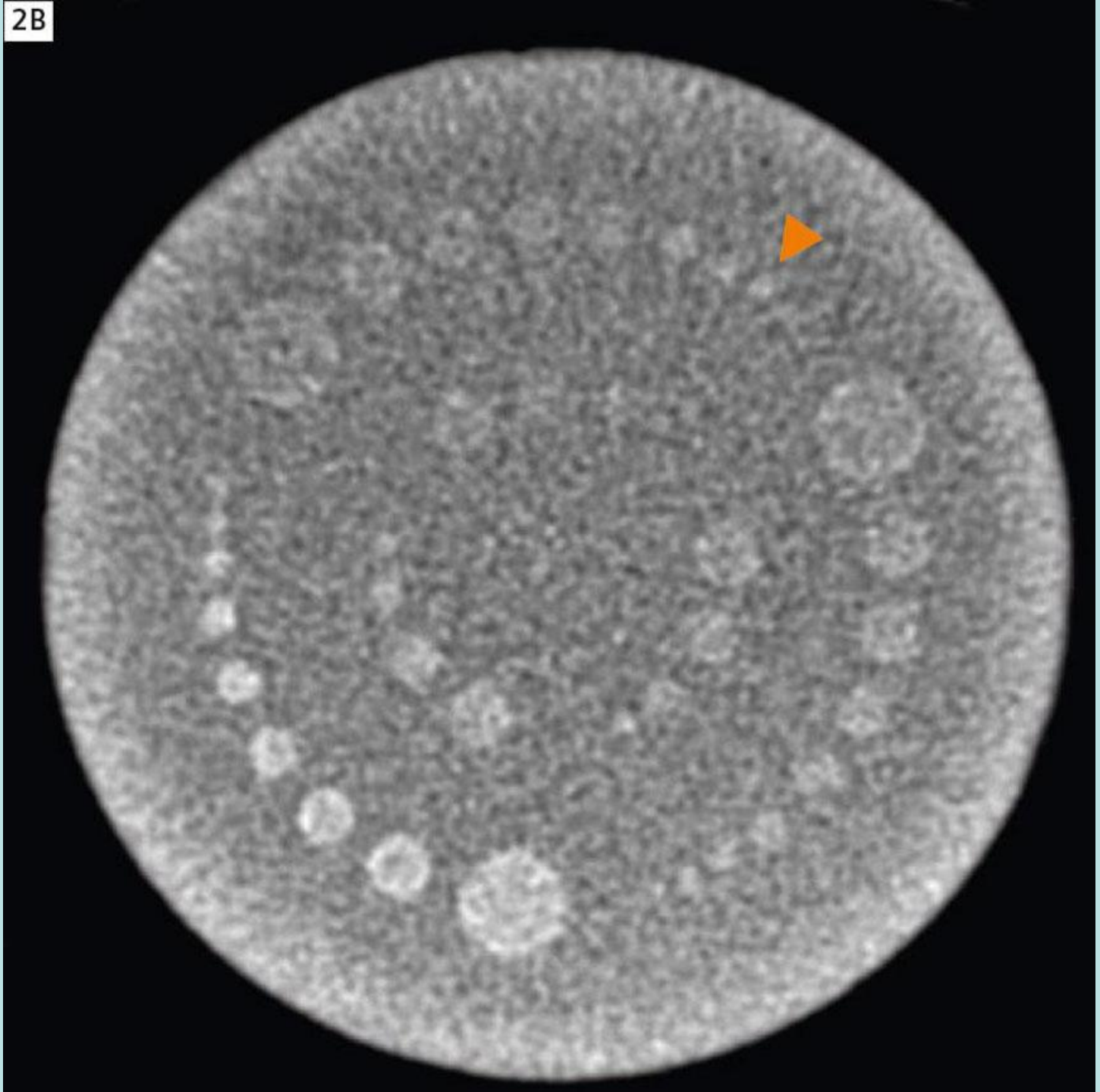
2B

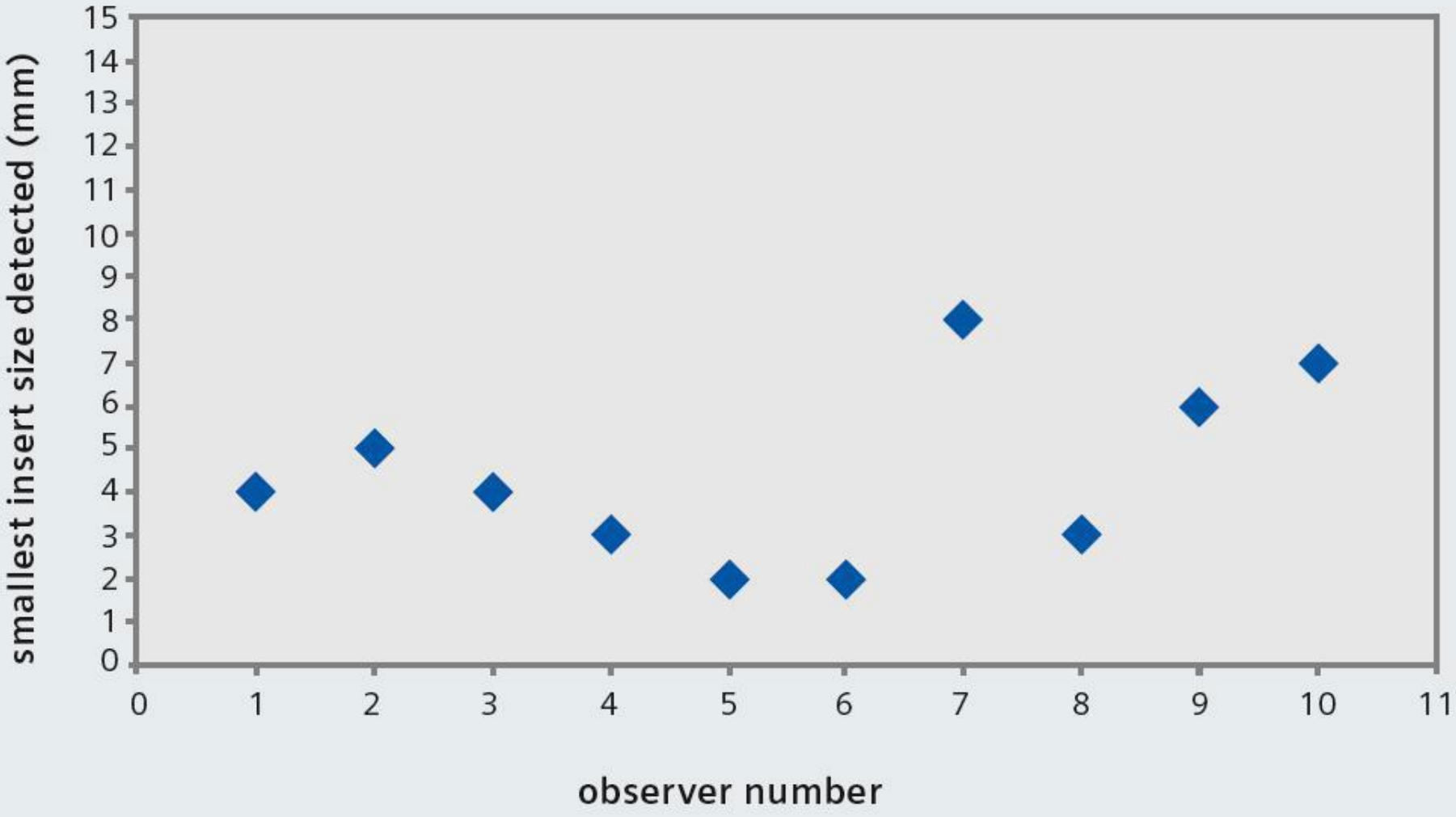
smallest insert size detected (mm)
15
14
13
12
11
10
9
8
7
6
5
4
3
2
1
0
0
1
2
3
4
5
6
7
8
9
10
11
observer number

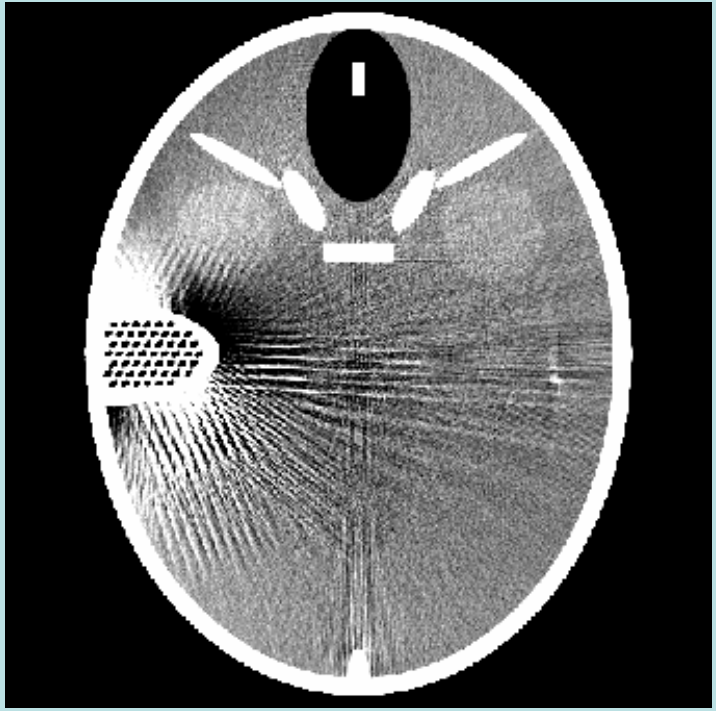

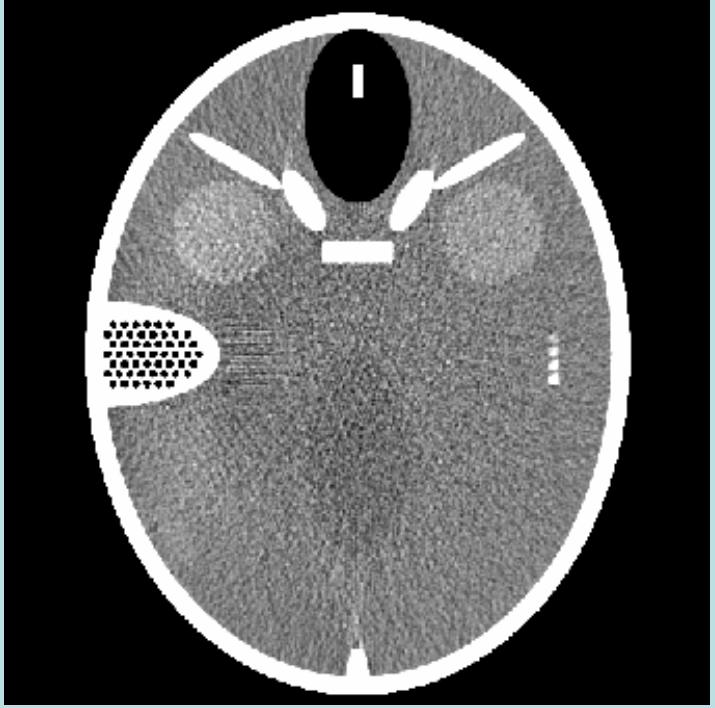

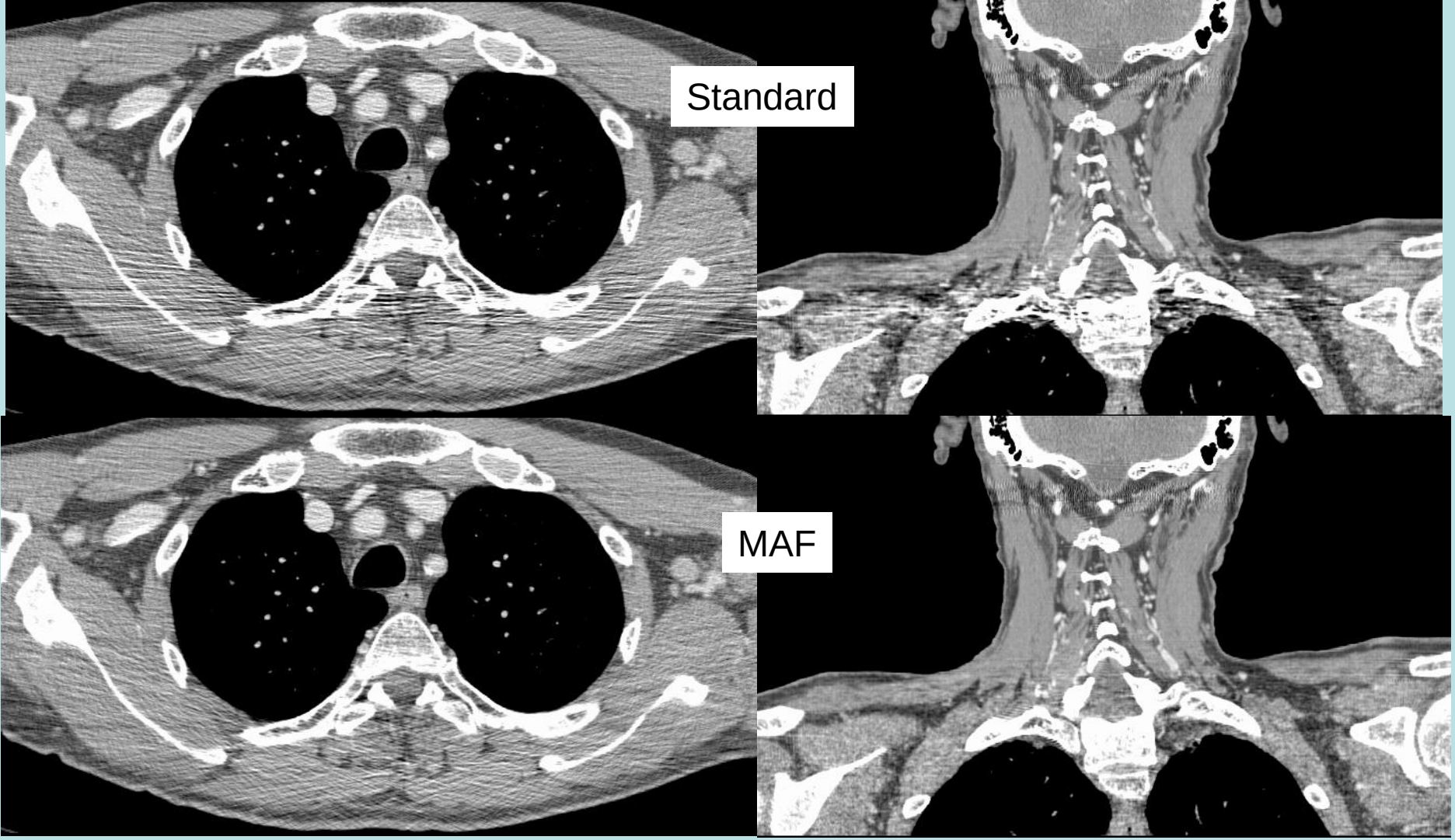
Standard
MAF

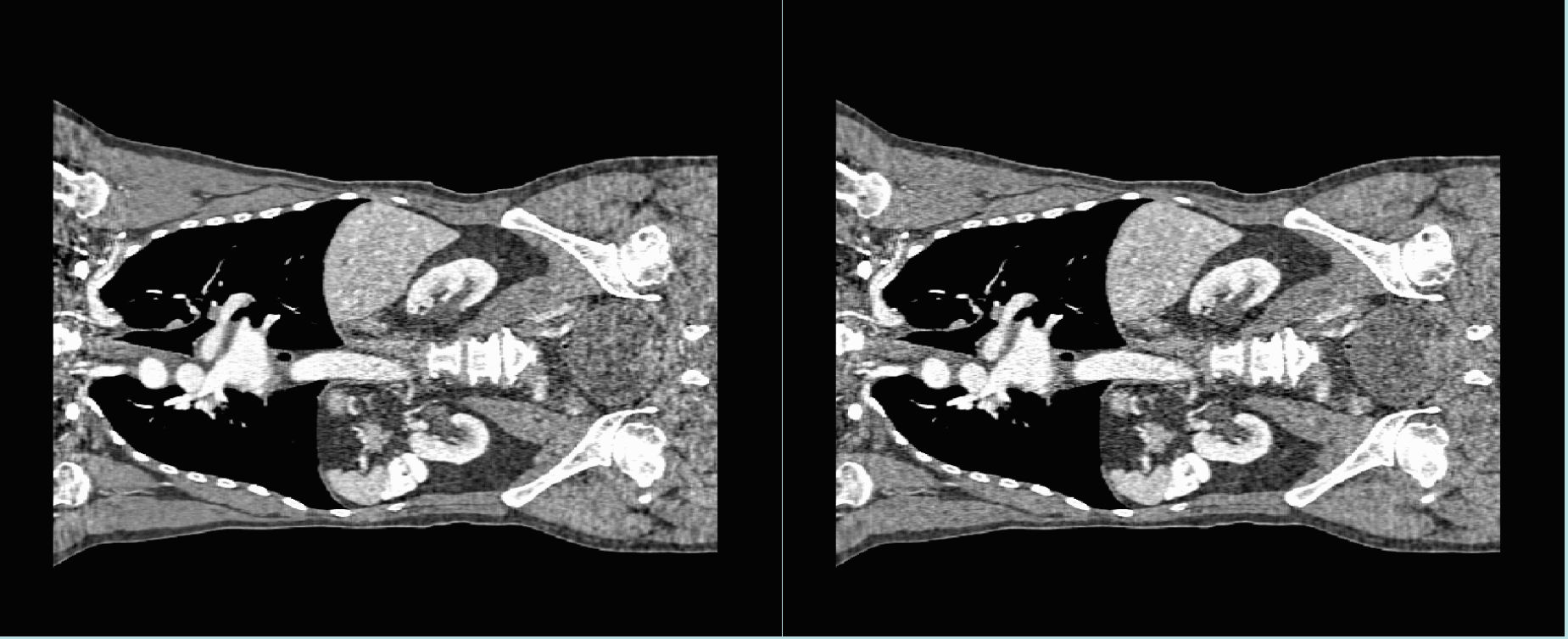

Automatska kontrola ekspozicije (AEC)

(z-os ovisna + angular dependent tube current modulation

34% mAs reduction with AEC at constant image quality for that specific case

Dose Reduction by Tube Current Modulation
Conventional scan: 327 mAs
Online current modulation: 166 mAs
53% dose reduction on average for the shoulder region
49% dose reduction in this case

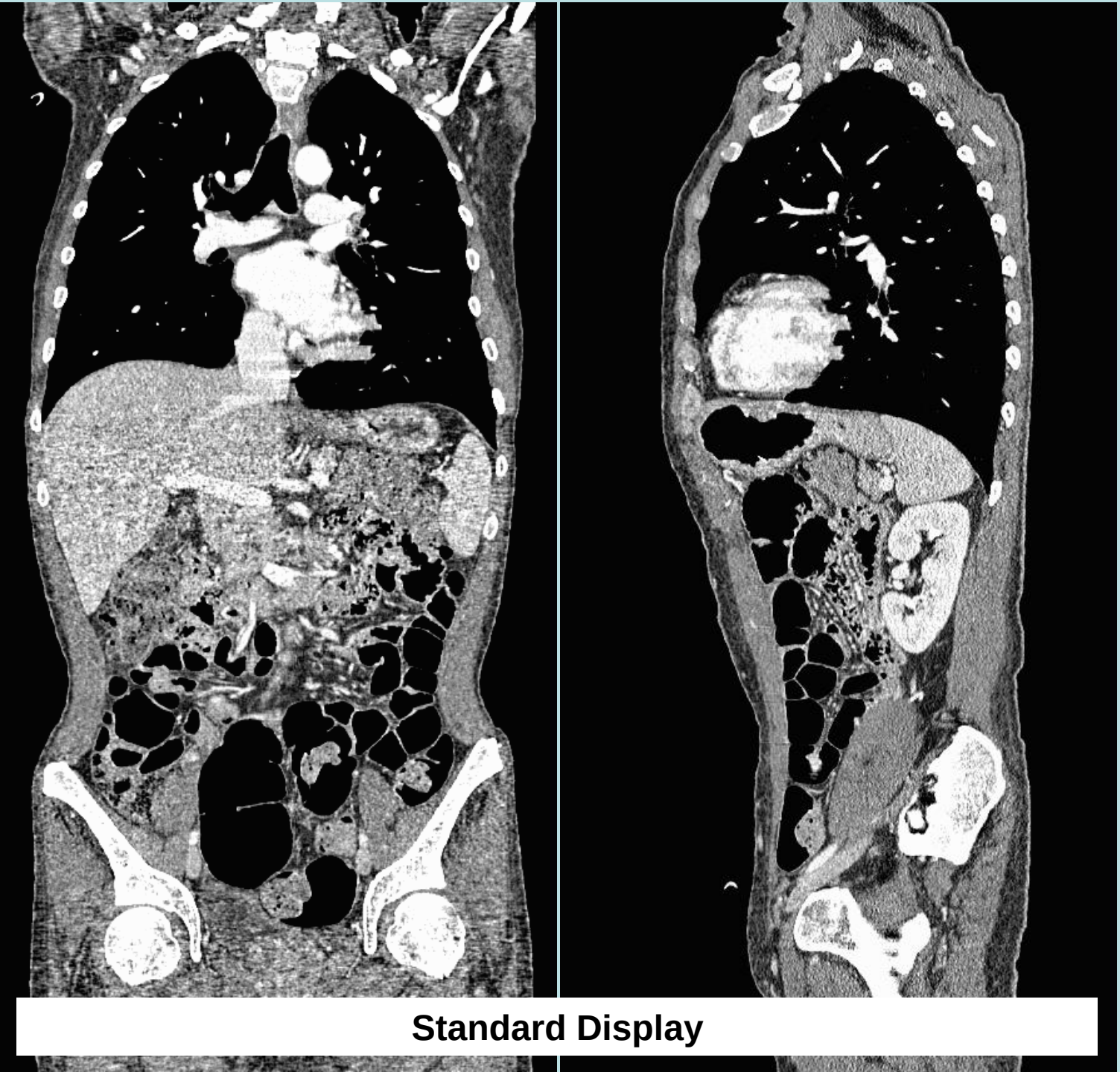

Standard Display

Sliding Thin Slab (STS) Display

Strategija smanjenja doze

Potencijalni razlozi porasta:
. Veliki volumen skeniranja
. Multifazno snimanje
. Više pretraga
. Velika prostorna rezolucija (tanki slojevi)
Nove specijalne aplikacije

Načini smanjenja doze:
. Nove tehnike display-a
. Napredni rekonstrukcijski algoritmi (MAF)
. Automatska kontrola ekspozicije (AEC)
. Optimiziran spektar
. Dose utor

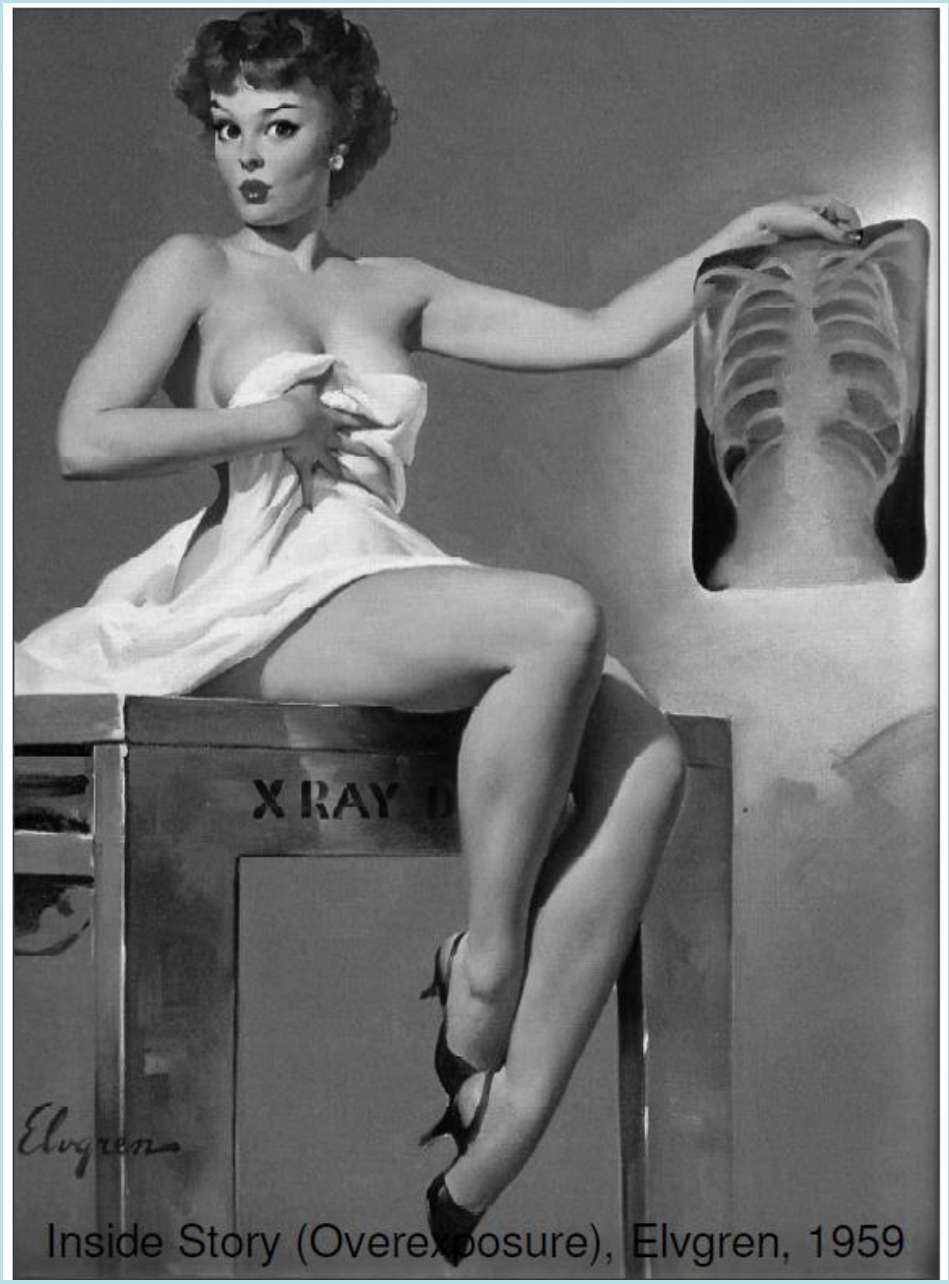

Inside Story (Overexposure), Elvgren, 1959